

Review

# Superconductivity in $\text{La}_2\text{O}_2\text{M}_4\text{S}_6$ -Type Bi-based Compounds: A Review on Element Substitution Effects

Rajveer Jha \* and Yoshikazu Mizuguchi 

Department of Physics, Tokyo Metropolitan University, 1-1 Minami-Osawa, Hachioji, Tokyo 192-0397, Japan; mizugu@tmu.ac.jp

\* Correspondence: rajveerjha@gmail.com

Received: 13 February 2020; Accepted: 5 April 2020; Published: 6 April 2020



**Abstract:** Since 2012, layered compounds containing Bi-*Ch* (*Ch*: S and Se) layers have been extensively studied in the field of superconductivity. The most-studied system is BiS<sub>2</sub>-based superconductors with two-layer-type conducting layers. Recently, superconductivity was observed in  $\text{La}_2\text{O}_2\text{M}_2\text{S}_6$  ( $M$  = metals), which contains four-layer-type conducting layers. The four-layer-type Bi-based superconductors are new systems in the family of Bi-based superconductors; we can expect further development of Bi-based layered superconductors. In this review article, we summarize the progress of synthesis, structural analysis, investigations on superconducting properties, and material design of the four-layer-type Bi-based superconductors. In-plane chemical pressure is the factor essential for the emergence of bulk superconductivity in the system. The highest  $T_c$  of 4.1 K was observed in Rare Earth elements (*RE*) substituted  $\text{La}_{2-x}\text{RE}_x\text{O}_2\text{Bi}_3\text{Ag}_{0.6}\text{Sn}_{0.4}\text{S}_6$ .

**Keywords:** Bi-based superconductors; layered superconductor; chemical pressure; substitution effect; superconducting phase diagram

## 1. Introduction

Many new superconductors with a layered structure have been synthesized since the discovery of cuprate high- $T_c$  ( $T_c$ : transition temperature) superconductor [1]. One of the big discoveries of a layered superconductor system is the discovery of Fe-based superconductors [2]. In addition, the BiS<sub>2</sub>-based layered superconductors are a recent example of layered superconductors [3,4]. The BiS<sub>2</sub>-based layered superconductors have tremendously attracted the condensed matter physics scientific community since 2012 [3–19]. The crystal structure of the BiS<sub>2</sub>-based compounds is generally composed of the BiS<sub>2</sub> layers as superconducting layers and insulating (blocking) layers like LaO, which is analogous to the structure of high- $T_c$  cuprates and Fe-based superconductors [1,2]. The first BiS<sub>2</sub>-based compound was Bi<sub>4</sub>O<sub>4</sub>S<sub>3</sub> with  $T_c$  (onset) = 8.6 K, later on,  $\text{LnO}_{1-x}\text{F}_x\text{BiS}_2$  ( $\text{Ln} = \text{La}, \text{Ce}, \text{Nd}, \text{Yb}, \text{Pr}$ ),  $\text{Sr}_{1-x}\text{La}_x\text{FBiS}_2$ , and  $\text{EuFBiS}_2$  with  $T_c$  of 2–11 K have been discovered [3–20]. Mainly, the crystal structure of  $\text{Ln}(\text{O},\text{F})\text{BiS}_2$  consists of blocking layers ( $\text{LnO}$ ) and the conducting layers ( $\text{BiS}_2$ ); the underlying crystal structure has been shown in Figure 1 [4]. Other materials similar to the BiS<sub>2</sub>-based layered compounds were developed by replacing S by Se. Therefore, these compounds have been called Bi*Ch*<sub>2</sub>-based compounds (*Ch* = S, Se) [21–45]. After the successful growth of single crystals of  $\text{LnO}_{1-x}\text{F}_x\text{BiS}_2$  phase, an important feature has been discussed in the crystal structure of the BiS<sub>2</sub>-based compound [46–48]. The single crystals of  $\text{LnO}_{1-x}\text{F}_x\text{BiS}_2$  can be easily exfoliated (layer by layer) because of the plate-like shape and the existence of a van der Waals gap between the BiS planes [46–48]. Notably, the van der Waals gap between two BiS planes became the essential feature when designing four-layer-type  $\text{La}_2\text{O}_2\text{M}_4\text{S}_6$  ( $M$ : metals) compounds [49–52], which is the central issue of this review article.

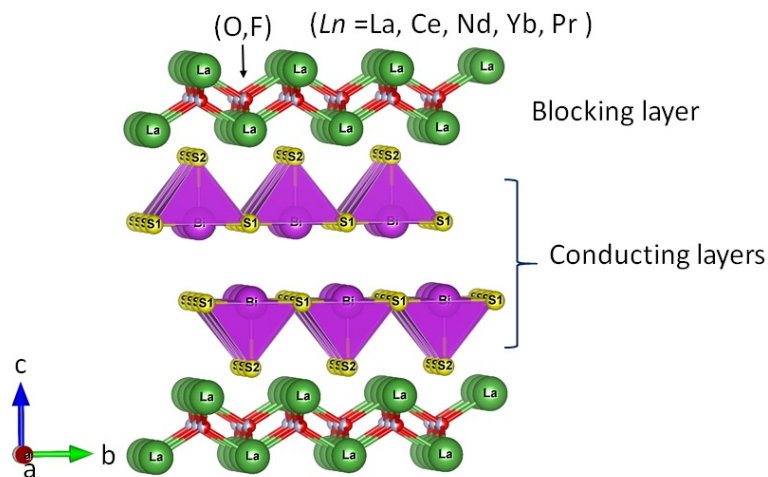


**Figure 1.** The crystal structure of the  $\text{BiS}_2$ -based  $\text{Ln}(\text{O},\text{F})\text{BiS}_2$  superconducting systems, the two  $\text{BiS}_2$  layers are conducting layers (CL), and  $\text{LnO}$  layers are Blocking layers (BL) [4].

The concept of designing new  $\text{BiS}_2$ -based compounds with a thicker (four-layer-type) superconducting layer can be related to the case of the high- $T_c$  cuprates [1,53–57]. The thickness of the superconducting layer was essential to achieve a higher  $T_c$  [53–57].  $T_c$  above 100 K has been achieved by increasing the number of  $\text{CuO}_2$  (conducting) layers in the unit cell of the crystal structure. We have assumed the same concept to develop  $\text{La}_2\text{O}_2\text{M}_4\text{S}_6$  four-layer type  $\text{BiS}_2$ -based superconductors.

The first cuprate superconductor,  $\text{La}_{2-x}\text{Ba}_x\text{CuO}_4$  (LBCO) with  $T_c = 30$  K was discovered in 1986 [1]. The  $T_c$  has increased up to 40 K for the  $\text{La}_{2-x}\text{Sr}_x\text{CuO}_4$  (LSCO) superconductor [54]. The structure of LBCO has been classified as  $\text{K}_2\text{NiF}_4$  (214)-type tetragonal. Soon after the discovery of the LBCO superconductors, the  $\text{YBa}_2\text{Cu}_3\text{O}_{7-\delta}$  (YBCO) superconductor with  $T_c = 93$  K has been discovered [53]. In the crystal structure of YBCO, there are two  $\text{CuO}_2$  planes [53]. The superconductivity in a more complex system  $\text{Bi}_2\text{Sr}_2\text{Ca}_2\text{Cu}_3\text{O}_x$  (BSCCO-2223) and  $\text{Bi}_2\text{Sr}_2\text{CaCu}_2\text{O}_x$  (BSCCO-2212) was discovered in 1988 with  $T_c = 110$  K and 96 K, respectively [55–58]. The common component in all the cuprates is the  $\text{CuO}_2$  planes. The LSCO, YBCO, and BSCCO-2223 compounds can be regarded as one-layer-type, two-layer-type, and three-layer-type structure among the cuprate family. It seems that (see Figure 2), the  $T_c$  of cuprates has been increased by increasing numbers of the  $\text{CuO}_2$  layers in the unit cell. This trend in cuprates may be expected for other layered superconductors.

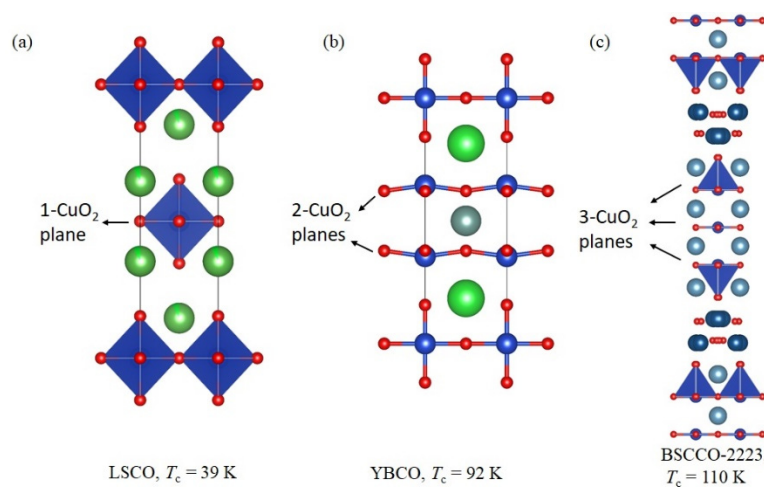


**Figure 2.** The crystal structure of High Temperature Superconductors (HTSC) family. (a)  $\text{La}_{2-x}\text{Sr}_x\text{CuO}_4$  (LSCO) [52], (b)  $\text{YBa}_2\text{Cu}_3\text{O}_{7-\delta}$  (YBCO) [51], and (c)  $\text{Bi}_2\text{Sr}_2\text{Ca}_2\text{Cu}_3\text{O}_x$  (BSCCO-2223) [55].

Since this review is focused on the four-layer-type BiS<sub>2</sub>-based compounds, a brief summary of the Bi-based compound is important to understand the four-layer-type compounds. Superconductivity in Bi-based compounds has been studied extensively. The highest  $T_c$  ever achieved for the Bi-2223 and 2212 compounds, the  $T_c$  most likely depends on the number of CuO<sub>2</sub> layers in the crystal structure of these compounds [55–58]. The pure Bi is superconducting under pressure because, at low temperature, the formation of high-pressure metallic phases of Bi and the  $T_c$  of these phases are 3.9–8.3 K [59–63]. At ambient pressure, Bi shows the superconductivity in amorphous Bi-thin films, Bi granular composite, and Bi thin films on the Ni substrates and  $T_c$  around 6.0 K, 5.5 K, and 4.0 K respectively [64–68]. In addition, superconductivity has been revealed in the Bi-based compounds like; (Ba/Sr)Bi<sub>3</sub> and BiNi<sub>3</sub>, and the  $T_c$  was nearly 5–6 K [69,70]. More recently, BiS<sub>2</sub>-based compounds have been discussed all-inclusive [3–12].

The continuous development of BiS<sub>2</sub>-based compounds has encouraged us to study the four-layer-type compounds [49–52]. Initially, the first four-layer-type LaOBiPbS<sub>3</sub> (equivalently described as La<sub>2</sub>O<sub>2</sub>Bi<sub>2</sub>Pb<sub>2</sub>S<sub>6</sub> to cover one unit cell) compound has been reported as a semiconductor and thermoelectric material [49]. Later on, the metal (*M*) site of La<sub>2</sub>O<sub>2</sub>M<sub>4</sub>S<sub>6</sub> has been modified as *M* = Bi<sub>3</sub>Ag, and the resultant compound was La<sub>2</sub>O<sub>2</sub>Bi<sub>3</sub>AgS<sub>6</sub> [51]. This newly designed oxychalcogenide La<sub>2</sub>O<sub>2</sub>Bi<sub>3</sub>AgS<sub>6</sub> showed metallic conductivity and superconductivity at  $T_c = 0.5$  K [52]. Previous studies on the two-layer-type (BiS<sub>2</sub>-based *Ln*O<sub>1-x</sub>F<sub>x</sub>BiS<sub>2</sub>) phase has suggested that the doping effect at the various sites of a compound induced bulk superconductivity or improve the superconducting properties [4–28,68–72], which has been understood by in-plane chemical pressure effects. Therefore, we could assume that the superconducting properties of La<sub>2</sub>O<sub>2</sub>Bi<sub>3</sub>AgS<sub>6</sub> may be improved by element substitutions. Then, we doped Sn for the Ag site and found that  $T_c$  increases up to 2.5 K in La<sub>2</sub>O<sub>2</sub>Bi<sub>3</sub>Ag<sub>0.6</sub>Sn<sub>0.4</sub>S<sub>6</sub> [73]. The in-plane chemical pressure (chemical pressure effect along *ab*-plane) was not sufficient in La<sub>2</sub>O<sub>2</sub>Bi<sub>3</sub>Ag<sub>0.6</sub>Sn<sub>0.4</sub>S<sub>6</sub>, and Se substitution at the S site achieved bulk superconductivity with a  $T_c$  of 3.5 K in La<sub>2</sub>O<sub>2</sub>Bi<sub>3</sub>Ag<sub>0.6</sub>Sn<sub>0.4</sub>S<sub>5.7</sub>Se<sub>0.3</sub> [73]. Furthermore, substitutions in the block layer of BiS<sub>2</sub>-based compounds could generate in-plane chemical pressure and induce bulk superconductivity as well [71]. Therefore, in-plane chemical pressure by Rare Earth (*RE*) ion substitution in the blocking layer of La<sub>2</sub>O<sub>2</sub>Bi<sub>3</sub>Ag<sub>0.6</sub>Sn<sub>0.4</sub>S<sub>6</sub> has been examined [74,75]. Bulk superconductivity has been induced by *RE* elements smaller than La, and  $T_c$  increased up to 4.0 K for the Eu-doped La<sub>2-x</sub>Eu<sub>x</sub>O<sub>2</sub>Bi<sub>3</sub>Ag<sub>0.6</sub>Sn<sub>0.4</sub>S<sub>6</sub> ( $x = 0.4$ ) compound [74]. Furthermore, we have doped Sm at the La site as well and observed bulk superconductivity at  $T_c = 4.1$  K in the La<sub>2-x</sub>Sm<sub>x</sub>O<sub>2</sub>Bi<sub>3</sub>Ag<sub>0.6</sub>Sn<sub>0.4</sub>S<sub>6</sub>. The trend on the correlation between  $T_c$  and crystal structure in *RE*O<sub>1-x</sub>F<sub>x</sub>BiS<sub>2</sub> superconductors has been found, and the importance of in-plane chemical pressure has been confirmed.

Recently, superconductivity in Bi<sub>3</sub>O<sub>2</sub>S<sub>2</sub>Cl at  $T_c = 2.8$  K has been reported by Ruan et al. As shown in Figure 3, this compound can be regarded as a one-layer-type Bi-based superconductor [76]. As mentioned earlier, the BiCh<sub>2</sub>-based systems like *RE*O<sub>1-x</sub>F<sub>x</sub>BiS<sub>2</sub> have two BiS<sub>2</sub> layers in a unit cell [4–31]. Therefore, the BiCh<sub>2</sub>-based system can be regarded as two-layer-type. Then, according to the categorization of conducting layer structure, we regard the structure of La<sub>2</sub>O<sub>2</sub>M<sub>4</sub>S<sub>6</sub> as four-layer-type as summarized in Figure 3. A similar strategy of cuprates, as mentioned in Figure 2, can be applied for the Bi-based compounds by changing constituent elements and the number of conducting layers to develop high  $T_c$  Bi-based superconductors.

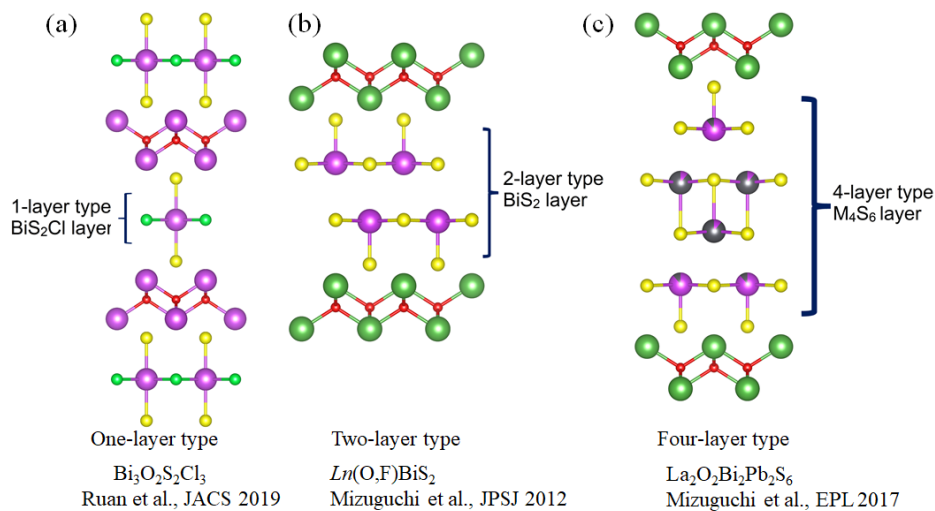


**Figure 3.** The crystal structure of Bi-based compounds (a) 1-layer type  $\text{Bi}_3\text{O}_2\text{S}_2\text{Cl}_3$  [76], (b) 2-layers type  $\text{Ln}(\text{O}, \text{F})\text{BiS}_2$  superconductors [4], and (c) 4-layers type  $\text{La}_2\text{O}_2\text{Bi}_2\text{Pb}_2\text{S}_6$  [51].

The in-plane chemical pressure appears in the two-layers  $\text{BiCh}_2$ -based, and four-layers type compounds can be regarded as a change in the lattice parameter  $a$ . Figure 4 shows the lattice parameter  $a$  dependence of  $T_c$  for 1-layer type  $\text{Bi}_3\text{O}_2\text{S}_2\text{Cl}_3$  [76], 2-layers type  $\text{Ln}(\text{O}, \text{F})\text{BiS}/\text{Se}_2$  superconductors, and 4-layers type  $\text{La}_2\text{O}_2\text{M}_4\text{S}_6$  compounds. With replacing  $\text{Ln}$  (La to Ce, Pr, Nd) in  $\text{Ln}(\text{O}, \text{F})\text{BiS}_2$ , the considerable change in lattice parameter  $a$  has been observed, which is changing the  $T_c$  largely of 2-layers type superconductors [3–12]. We notice that a slight change in the lattice parameter  $a$  is creating a large effect on the superconductivity on 4-layers-type  $\text{La}_2\text{O}_2\text{M}_4\text{S}_6$  compounds [52,73–75].

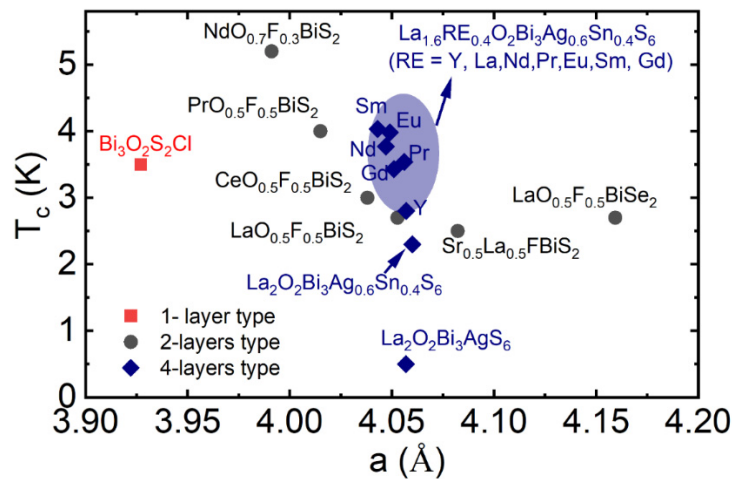


**Figure 4.** The  $T_c$  vs. lattice parameter  $a$ , for 1-layer type, 2-layers type, and 4-layers type crystal structure of Bi-based compounds the data extract from references [3–12,52,73–78].

In this review article, we summarize the evolution of  $T_c$  in Table 1. Table 1 contains the change in  $T_c$  with the change of doping elements on various sites  $RE$ ,  $M$ , and  $S$  of  $\text{La}_2\text{O}_2\text{M}_4\text{S}_6$ , four-layers-type  $\text{BiS}_2$ -based compounds [52,73–78].

**Table 1.** Four-layer-type superconductors with  $T_c$  and references.

Materials	$T_c$ (K)	Ref.
$\text{La}_2\text{O}_2\text{Bi}_3\text{AgS}_6$	0.5	[52]
$\text{La}_2\text{O}_2\text{Bi}_3\text{Ag}_{0.9}\text{In}_{0.1}\text{S}_6$	0.45	
$\text{La}_2\text{O}_2\text{Bi}_3\text{Ag}_{0.8}\text{In}_{0.2}\text{S}_6$	0.42	[78]
$\text{La}_2\text{O}_2\text{Bi}_3\text{Ag}_{0.7}\text{In}_{0.3}\text{S}_6$	0.4	
$\text{La}_2\text{O}_2\text{Bi}_3\text{Ag}_{0.6}\text{In}_{0.4}\text{S}_6$	0.4	
$\text{La}_2\text{O}_2\text{Bi}_3\text{Ag}_{0.9}\text{Sn}_{0.1}\text{S}_6$	0.55	
$\text{La}_2\text{O}_2\text{Bi}_3\text{Ag}_{0.8}\text{Sn}_{0.2}\text{S}_6$	0.95	
$\text{La}_2\text{O}_2\text{Bi}_3\text{Ag}_{0.7}\text{Sn}_{0.3}\text{S}_6$	1.83	[73]
$\text{La}_2\text{O}_2\text{Bi}_3\text{Ag}_{0.6}\text{Sn}_{0.4}\text{S}_6$	2.5	
$\text{La}_2\text{O}_2\text{Bi}_3\text{Ag}_{0.5}\text{Sn}_{0.5}\text{S}_6$	1.7	
$\text{La}_2\text{O}_2\text{Bi}_3\text{Ag}_{0.6}\text{Sn}_{0.4}\text{S}_{5.7}\text{Se}_{0.3}$	3.0	
$\text{La}_{1.9}\text{Eu}_{0.1}\text{O}_2\text{Bi}_3\text{Ag}_{0.6}\text{Sn}_{0.4}\text{S}_6$	2.84	
$\text{La}_{1.8}\text{Eu}_{0.2}\text{O}_2\text{Bi}_3\text{Ag}_{0.6}\text{Sn}_{0.4}\text{S}_6$	3.26	
$\text{La}_{1.7}\text{Eu}_{0.3}\text{O}_2\text{Bi}_3\text{Ag}_{0.6}\text{Sn}_{0.4}\text{S}_6$	3.64	[74]
$\text{La}_{1.6}\text{Eu}_{0.4}\text{O}_2\text{Bi}_3\text{Ag}_{0.6}\text{Sn}_{0.4}\text{S}_6$	4.0	
$\text{La}_{1.5}\text{Eu}_{0.5}\text{O}_2\text{Bi}_3\text{Ag}_{0.6}\text{Sn}_{0.4}\text{S}_6$	3.63	
$\text{La}_{1.4}\text{Eu}_{0.6}\text{O}_2\text{Bi}_3\text{Ag}_{0.6}\text{Sn}_{0.4}\text{S}_6$	3.58	
$\text{La}_{1.9}\text{Sm}_{0.1}\text{O}_2\text{Bi}_3\text{Ag}_{0.6}\text{Sn}_{0.4}\text{S}_6$	2.89	
$\text{La}_{1.8}\text{Sm}_{0.2}\text{O}_2\text{Bi}_3\text{Ag}_{0.6}\text{Sn}_{0.4}\text{S}_6$	3.345	
$\text{La}_{1.7}\text{Sm}_{0.3}\text{O}_2\text{Bi}_3\text{Ag}_{0.6}\text{Sn}_{0.4}\text{S}_6$	3.795	To be published
$\text{La}_{1.6}\text{Sm}_{0.4}\text{O}_2\text{Bi}_3\text{Ag}_{0.6}\text{Sn}_{0.4}\text{S}_6$	4.1	
$\text{La}_{1.5}\text{Sm}_{0.5}\text{O}_2\text{Bi}_3\text{Ag}_{0.6}\text{Sn}_{0.4}\text{S}_6$	3.867	
$\text{La}_{1.4}\text{Sm}_{0.6}\text{O}_2\text{Bi}_3\text{Ag}_{0.6}\text{Sn}_{0.4}\text{S}_6$	3.59	
$\text{La}_{1.6}\text{Y}_{0.4}\text{O}_2\text{Bi}_3\text{Ag}_{0.6}\text{Sn}_{0.4}\text{S}_6$	2.68	
$\text{La}_{1.6}\text{Pr}_{0.4}\text{O}_2\text{Bi}_3\text{Ag}_{0.6}\text{Sn}_{0.4}\text{S}_6$	3.54	[74]
$\text{La}_{1.6}\text{Nd}_{0.4}\text{O}_2\text{Bi}_3\text{Ag}_{0.6}\text{Sn}_{0.4}\text{S}_6$	3.8	
$\text{La}_{1.6}\text{Gd}_{0.4}\text{O}_2\text{Bi}_3\text{Ag}_{0.6}\text{Sn}_{0.4}\text{S}_6$	3.46	
$\text{LaPrO}_2\text{Bi}_3\text{Ag}_{0.6}\text{Sn}_{0.4}\text{S}_6$	3.5	[75]
$\text{LaNdO}_2\text{Bi}_3\text{Ag}_{0.6}\text{Sn}_{0.4}\text{S}_6$	3.4	
$\text{La}_2\text{O}_2\text{Bi}_2\text{PbS}_{5.5}\text{Se}_{0.5}$	1.15	[77]
$\text{La}_2\text{O}_2\text{Bi}_2\text{PbS}_{5.0}\text{Se}_{1.0}$	1.9	

## 2. The Crystal Structure of $\text{La}_2\text{O}_2\text{M}_4\text{S}_6$ Type Four-Layer Compounds

### 2.1. $\text{La}_2\text{O}_2\text{Bi}_2\text{Pb}_2\text{S}_6$

Primarily, the  $\text{La}_2\text{O}_2\text{Bi}_2\text{Pb}_2\text{S}_6$  compound was synthesized and reported as thermoelectric material by Sun et al. [49].  $\text{La}_2\text{O}_2\text{Bi}_2\text{Pb}_2\text{S}_6$  is composed of  $\text{Bi}_2\text{Pb}_2\text{S}_6$  conducting layers and LaO block layers.  $\text{La}_2\text{O}_2\text{Bi}_2\text{Pb}_2\text{S}_6$  has a tetragonal structure with space group  $P4/nmm$ , as shown in Figure 5. We further investigated the site selectivity at the  $M$  ( $=\text{Bi}_2\text{Pb}_2$ ) site and performed band calculations [50]. From synchrotron X-ray and neutron diffraction, we revealed that the  $M_4\text{S}_6$  layers were almost ordered into Bi- and Pb-rich sites. According to our study, the structure could be rather regarded as stacks of LaOBiS<sub>2</sub>-type and rock-salt-type (PbS-type) layers; a schematic image of the crystal structure of  $\text{La}_2\text{O}_2\text{Bi}_2\text{Pb}_2\text{S}_6$  is shown in Figure 5.

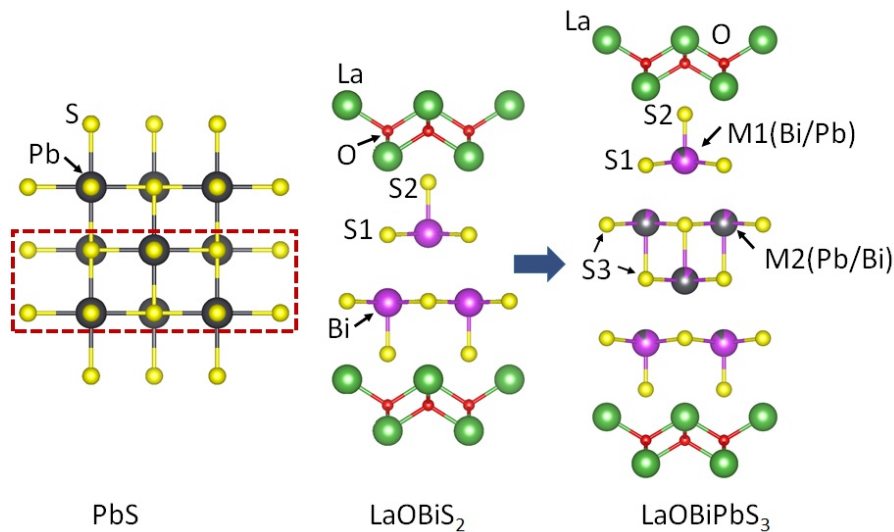


**Figure 5.** The schematic unit cell of  $\text{La}_2\text{O}_2\text{Bi}_2\text{Pb}_2\text{S}_6$  with the relationship of the crystal structure between PbS (rock-salt-type),  $\text{LaOBiS}_2$ , and  $\text{LaOBiPbS}_3$  [50].

### 2.2. $\text{La}_2\text{O}_2\text{Bi}_3\text{AgS}_6$

The concept of structural (stacking) in  $\text{La}_2\text{O}_2\text{Bi}_2\text{Pb}_2\text{S}_6$  was taken to synthesize new phase  $\text{La}_2\text{O}_2\text{Bi}_3\text{AgS}_6$ , which was initially reported as a non-superconducting compound [51]. In  $\text{La}_2\text{O}_2\text{Bi}_3\text{AgS}_6$ , the (Ag, Bi)S layer was inserted in between two  $\text{BiS}_2$  layers of the  $\text{LaOBiS}_2$  in place of the PbS layer in  $\text{La}_2\text{O}_2\text{Bi}_2\text{Pb}_2\text{S}_6$  [51]. It is worth noting that the interlayer distance M2-S1 is clearly different between  $M = \text{Bi}_2\text{Pb}_2$  and  $M = \text{Bi}_3\text{Ag}$ . The structural difference affects physical properties in those compounds, which will be shown in the following parts.

### 2.3. Available Elements for RE, M, and S Sites of $\text{La}_2\text{O}_2\text{M}_4\text{S}_6$

Figure 6a shows the crystal structure for  $\text{La}_2\text{O}_2\text{Bi}_2\text{Pb}_2\text{S}_6$ . The substitution effect has been studied for the  $\text{La}_2\text{O}_2\text{Bi}_2\text{Pb}_2\text{S}_6$  compound, and different metals like Cd, Sn, and Sb have doped at the Pb (M2) site. The Se can partially substitute at the S (S1 and S3) site of  $\text{La}_2\text{O}_2\text{Bi}_2\text{Pb}_2\text{S}_6$ .

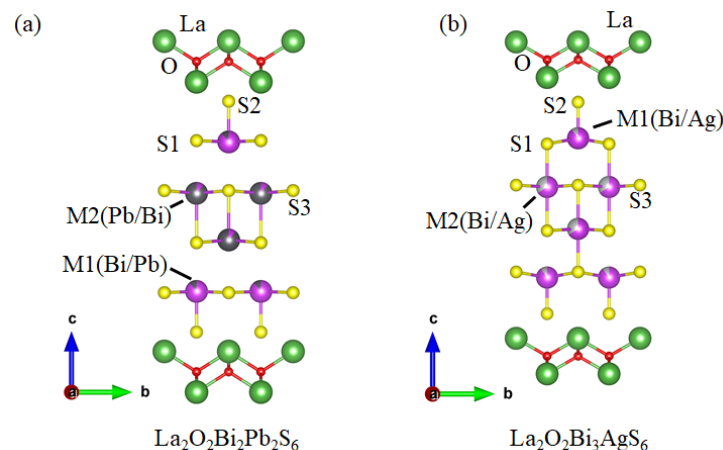


**Figure 6.** The schematic unit cell of (a)  $\text{La}_2\text{O}_2\text{Bi}_2\text{Pb}_2\text{S}_6$ ; (b)  $\text{La}_2\text{O}_2\text{Bi}_3\text{AgS}_6$  [50,51].

Figure 6b displays the crystal structure of  $\text{La}_2\text{O}_2\text{Bi}_3\text{AgS}_6$ .  $\text{La}_2\text{O}_2\text{Bi}_3\text{AgS}_6$  is a superconductor of  $T_c = 0.5$  K [52]. To increase the  $T_c$  and induce the bulk superconductivity, various sites of  $\text{La}_2\text{O}_2\text{Bi}_3\text{AgS}_6$  can be doped. The available elements for La sites are different REs like Eu, Sm, Pr, Nd, Y, and Gd. The In and Sn can be doped at the Ag (M2) site of  $\text{La}_2\text{O}_2\text{Bi}_3\text{AgS}_6$ . In addition, the S (S1 and S3) site can be partially substituted by Se of  $\text{La}_2\text{O}_2\text{Bi}_3\text{AgS}_6$ .

To summarize, so far, we could use  $M = \text{Bi, Pb, Ag, Sn, Cd, Sb, and In}$ ,  $RE = \text{La, Pr, Nd, Sm, Eu, and Gd}$ , and  $Ch = \text{S and Se}$  to synthesize the new four-layer-type Bi-based compounds.

### 3. Physical Properties of $\text{La}_2\text{O}_2\text{M}_4\text{S}_6$ ( $M = \text{Pb, Ag}$ )

#### 3.1. $\text{La}_2\text{O}_2\text{Bi}_2\text{Pb}_2\text{S}_6$ ; Doping Effect of Cd, Sn, and Sb at Pb Site

Since the data for  $\text{La}_2\text{O}_2\text{Bi}_2\text{Pb}_{2-x}\text{Cd}_x\text{S}_6$ ,  $\text{La}_2\text{O}_2\text{Bi}_2\text{Pb}_{2-x}\text{Sn}_x\text{S}_6$ , and  $\text{La}_2\text{O}_2\text{Bi}_2\text{Pb}_{2-x}\text{Sb}_x\text{S}_6$  have not been published in other journals, and has appeared in this paper for the first time, we summarized experimental details in the final section of this article.

The  $\text{La}_2\text{O}_2\text{Bi}_2\text{Pb}_2\text{S}_6$  compound has been reported as a narrow-gap semiconductor with an activation energy of  $\sim 17$  meV, confirmed by electrical resistivity and Hall effect measurements [49]. Moreover, the band calculations predicted that  $\text{La}_2\text{O}_2\text{Bi}_2\text{Pb}_2\text{S}_6$  was close to a zero-gap semiconductor (or metal), which is a clear difference from the electronic structure of the parent phase of the  $\text{BiCh}_2$ -based (two-layer-type) systems [3]. Experimentally obtained samples of  $\text{La}_2\text{O}_2\text{Bi}_2\text{Pb}_2\text{S}_6$ , however, showed insulating behavior in the electrical resistivity measurements at low temperatures [49,50]. Therefore, we have investigated the substitution effects of the Pb site with Cd, Sn, and Sb in  $\text{La}_2\text{O}_2\text{Bi}_2\text{Pb}_2\text{S}_6$ . Our motivation of the Pb-site substitution was to enhance the charge carriers and/or charge mobility by the substitution effects, but all the Pb-site substitutions resulted in insulating transport properties, while the insulating behavior has been somehow suppressed by the substitutions. Figure 7a–c shows the temperature dependences of electrical resistivity  $\rho(T)$  for the Cd-, Sn-, and Sb-doped  $\text{La}_2\text{O}_2\text{Bi}_2\text{Pb}_2\text{S}_6$ ; insets are the  $\log \rho$  vs.  $T$ . Unfortunately, we did not observe superconductivity by doping with Cd, Sn, and Sb.

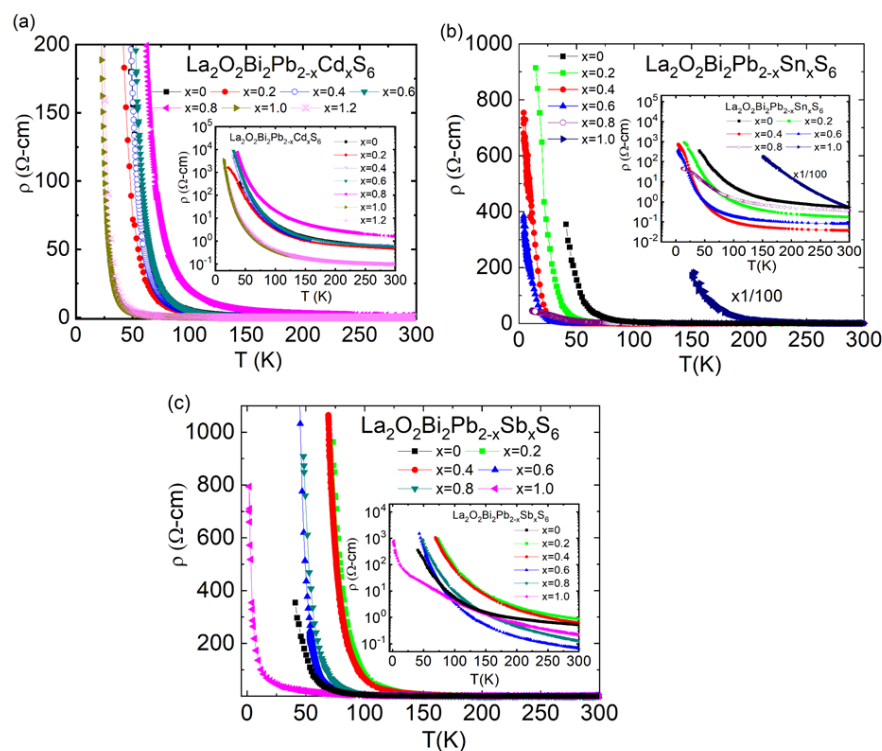


**Figure 7.** The temperature dependence of the electrical resistivity  $\rho(T)$  for (a) the  $\text{La}_2\text{O}_2\text{Bi}_2\text{Pb}_{2-x}\text{Cd}_x\text{S}_6$ , inset is the  $\log \rho$  vs.  $T$  for the  $\text{La}_2\text{O}_2\text{Bi}_2\text{Pb}_{2-x}\text{Cd}_x\text{S}_6$ . (b) the  $\text{La}_2\text{O}_2\text{Bi}_2\text{Pb}_{2-x}\text{Sn}_x\text{S}_6$  and inset is the  $\log \rho$  vs.  $T$  for the  $\text{La}_2\text{O}_2\text{Bi}_2\text{Pb}_{2-x}\text{Sn}_x\text{S}_6$ . (c) the  $\text{La}_2\text{O}_2\text{Bi}_2\text{Pb}_{2-x}\text{Sb}_x\text{S}_6$  and inset is the  $\log \rho$  vs.  $T$  for  $\text{La}_2\text{O}_2\text{Bi}_2\text{Pb}_{2-x}\text{Sb}_x\text{S}_6$ .

### 3.2. Superconductivity in Se-Doped $\text{La}_2\text{O}_2\text{Bi}_2\text{Pb}_2\text{S}_{6-x}\text{Se}_x$

Superconductivity has been observed for Se-substitution  $\text{La}_2\text{O}_2\text{Bi}_2\text{Pb}_2\text{S}_{6-x}\text{Se}_x$  [77]. Undoped  $\text{La}_2\text{O}_2\text{Bi}_2\text{Pb}_2\text{S}_6$  shows insulating behavior at low temperatures, but a partial substitution of S by Se induces metallicity in  $\text{La}_2\text{O}_2\text{Bi}_2\text{Pb}_2\text{S}_{6-x}\text{Se}_x$  [77]. We have confirmed that the lattice parameter  $a$  slightly expanded by the substitution effects of Se for the S site in  $\text{La}_2\text{O}_2\text{Bi}_2\text{Pb}_2\text{S}_{6-x}\text{Se}_x$ , which is an indication of the presence of in-plane chemical pressure effects in  $\text{La}_2\text{O}_2\text{Bi}_2\text{Pb}_2\text{S}_{6-x}\text{Se}_x$  due to Se substitutions. We observed superconductivity in  $\text{La}_2\text{O}_2\text{Bi}_2\text{Pb}_2\text{S}_{6-x}\text{Se}_x$ . The estimated transition temperatures are  $T_c = 1.15$  K for  $x = 0.5$  and  $T_c = 1.9$  K for  $x = 1.0$  [77].

### 3.3. Superconductivity in $\text{La}_2\text{O}_2\text{Bi}_3\text{AgS}_6$

Initially,  $\text{La}_2\text{O}_2\text{Bi}_3\text{AgS}_6$  was synthesized and reported as a non-superconducting compound [51]. Through optimization of synthesis condition to get a high quality  $\text{La}_2\text{O}_2\text{Bi}_3\text{AgS}_6$  sample, we obtained a sample which shows metallic conductivity and superconductivity at 0.5 K (see Figure 8a,b) [52].  $\text{La}_2\text{O}_2\text{Bi}_3\text{AgS}_6$  shows a charge density wave (CDW)-like transition at temperature ( $T^*$ ) in the  $\rho(T)$  curve below 180 K, which is similar to the case of  $\text{EuFBiS}_2$  [15]. We measured the  $\rho(T)$  by using an adiabatic demagnetization refrigerators (ADR) system down to the  $T = 0.1$  K. Superconductivity at  $T_c$  (onset) = 0.66 K has been observed in  $\text{La}_2\text{O}_2\text{Bi}_3\text{AgS}_6$  [52].  $\text{La}_2\text{O}_2\text{Bi}_3\text{AgS}_6$  was the first superconductor among  $\text{La}_2\text{O}_2\text{M}_4\text{S}_6$ -type (four-layer-type) Bi-based layered compounds.

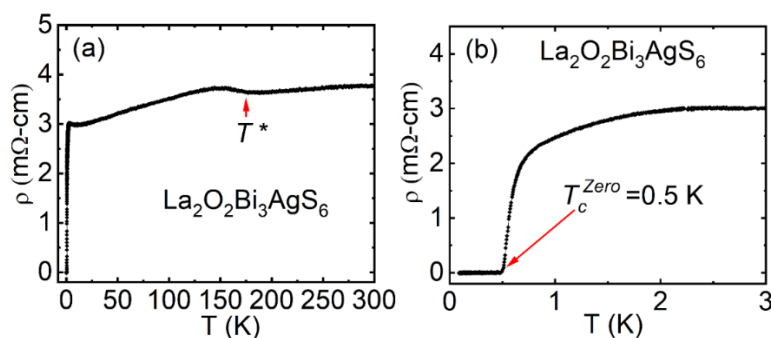


**Figure 8.** (color online) (a) The  $\rho(T)$  from 300-0.1K for the  $\text{La}_2\text{O}_2\text{Bi}_3\text{AgS}_6$  compound, hump in the  $\rho(T)$  curve denoted as  $T^*$ , Inset is the schematic unit cell of  $\text{La}_2\text{O}_2\text{Bi}_3\text{AgS}_6$ . (b) The zoomed view of the  $\rho(T)$  curve near  $T_c$  in the temperature range 3.0–0.1 K. Reproduced from J. Phys. Soc. Jpn. 87, 083704 (2018) [52], copyrighted by the Physical Society of Japan.

#### 3.3.1. Effect of In Doping in $\text{La}_2\text{O}_2\text{Bi}_3\text{Ag}_{1-x}\text{In}_x\text{S}_6$

Initially, we had tried to modify the conducting layers of the  $\text{La}_2\text{O}_2\text{Bi}_3\text{AgS}_6$  compound by substituting Ag by In [69]. The  $\rho(T)$  curve for  $\text{La}_2\text{O}_2\text{Bi}_3\text{Ag}_{1-x}\text{In}_x\text{S}_6$  from 300 – 0.4 K has been shown in Figure 9a; expanded view near the superconducting transition temperature range is shown in Figure 9b. The In-doped  $\text{La}_2\text{O}_2\text{Bi}_3\text{Ag}_{1-x}\text{In}_x\text{S}_6$  shows that the  $T_c$  slightly decreases with increasing In doping level. In contrast, the anomaly temperature of the CDW-like transition  $T^*$  did not change, although it was expected that the CDW-like transition is suppress by doping carrier. Figure 9c exhibits the  $T$  vs.  $x$  for  $\text{La}_2\text{O}_2\text{Bi}_3\text{Ag}_{1-x}\text{In}_x\text{S}_6$ , i.e.,  $x$ - $T$  phase diagram, which shows the change in superconducting transition  $T_c$  (zero) as a function of In doping level [78].  $T^*$  does not change with increasing  $x$ . The  $T_c$  slightly decreases with increasing  $x$  in  $\text{La}_2\text{O}_2\text{Bi}_3\text{Ag}_{1-x}\text{In}_x\text{S}_6$ . The decrease in  $T_c$  for the In-doped samples might be caused by the introduced disorder at the  $M$  site and the robustness of the CDW-like ordering ( $T^*$ ) against the In doping. A comparatively similar situation has been reported for the  $\text{NbSe}_{2-x}\text{Te}_x$ ; the  $T_c$  was decreasing by doping of Te at the Se site [79]. The structural analysis showed that the lattice parameters increasing with increasing In doping, which suggests the in-plane interaction is somehow decreasing.



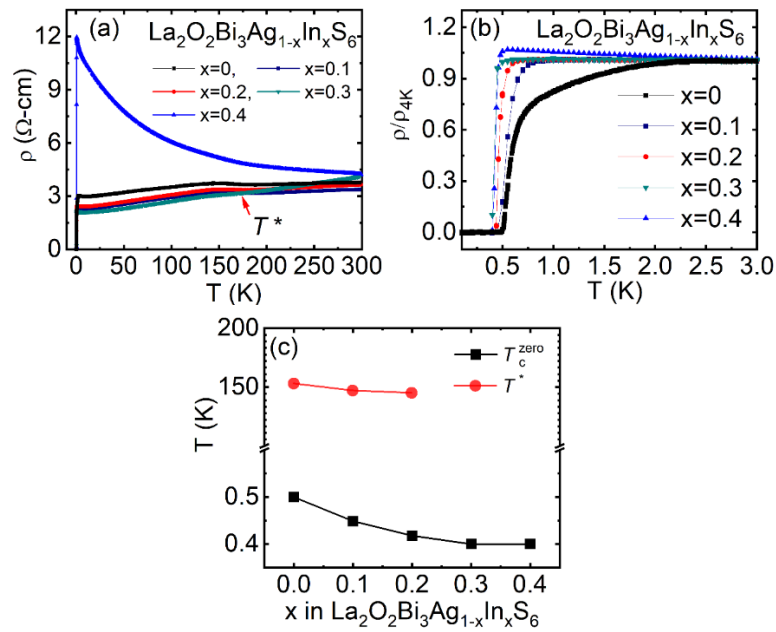


**Figure 9.** (color online) (a) The  $\rho(T)$  from 300–0.1 K for the  $\text{La}_2\text{O}_2\text{Bi}_3\text{Ag}_{1-x}\text{In}_x\text{S}_6$  ( $x = 0\text{--}0.4$ ) compounds. (b) The normalized  $\rho(T)/\rho(4\text{ K})$  curve in the temperature range 3.0–0.1 K. (c) The  $x$  dependence of  $T_c$  for  $\text{La}_2\text{O}_2\text{Bi}_3\text{Ag}_{1-x}\text{In}_x\text{S}_6$  ( $x = 0\text{--}0.4$ ) compounds and  $T^*$  scaled on the  $x$ - $T$  phase diagram for  $\text{La}_2\text{O}_2\text{Bi}_3\text{Ag}_{1-x}\text{In}_x\text{S}_6$ . CDW and SC symbolize as charge density wave and superconductivity, respectively. Reproduced from J. Phys.: Conf. Ser. **1293**, 012001 (2019) [78], copyrighted by the IOP Publishing Ltd.

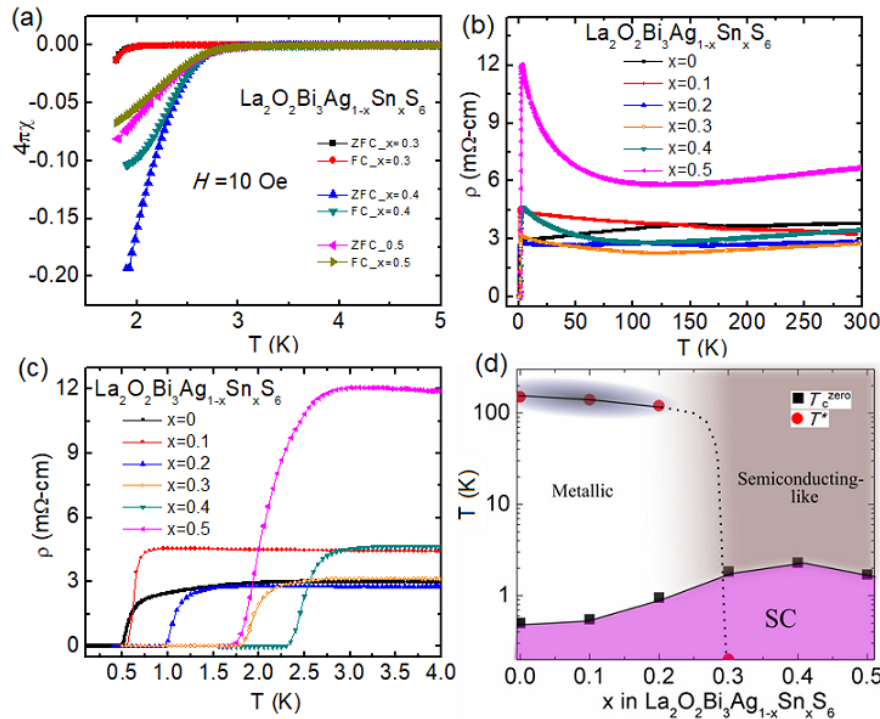
### 3.3.2. Sn-Substitution Effect in $\text{La}_2\text{O}_2\text{Bi}_3\text{Ag}_{1-x}\text{Sn}_x\text{S}_6$

We have substituted Ag at the  $M2$  site of  $\text{La}_2\text{O}_2\text{Bi}_3\text{AgS}_6$  by Sn [73]. The Sn substitution improved superconducting properties, and the maximum  $T_c$  was 2.5 K for the  $x = 0.4$  in  $\text{La}_2\text{O}_2\text{Bi}_3\text{Ag}_{1-x}\text{Sn}_x\text{S}_6$  [73]. Figure 10a–c shows the superconducting transitions in the temperature dependences of magnetization  $\chi(T)$  and resistivity  $\rho(T)$ . Figure 10d is the phase diagram for  $\text{La}_2\text{O}_2\text{Bi}_3\text{Ag}_{1-x}\text{Sn}_x\text{S}_6$ :  $T_c$  and  $T^*$  are plotted as a function of Sn concentration  $x$ . In  $\text{La}_2\text{O}_2\text{Bi}_3\text{AgS}_6$ , anomalies have been observed in the  $\rho(T)$ . Although In doping could not suppress the anomaly, the anomaly temperature  $T^*$  shifted to a lower temperature by Sn substitution. Finally, the anomaly disappeared at  $x = 0.3$ . Generally, CDW ordering can be expected to be suppressed by an increase in charge carriers or introduction of disorder in the lattice. As a result,  $T_c$  increases by the suppression of CDW temperature in materials in which superconductivity and CDW ordering coexist [80]. The magnitude of the Seebeck coefficient slightly decreased by Sn substitution, i.e., amount of electron charge carriers increased. Therefore, increased charge carrier would have suppressed anomaly temperature  $T^*$ . At the same time, Sn substitution should increase randomness at the  $M2$  site. Therefore, the increase in  $T_c$  in the present phase  $\text{La}_2\text{O}_2\text{Bi}_3\text{Ag}_{1-x}\text{Sn}_x\text{S}_6$  would be achieved by an increase in electron carriers and the introduced disorder at the  $M2$  site.

### 3.3.3. Se-Substitution Effect in $\text{La}_2\text{O}_2\text{Bi}_3\text{Ag}_{0.6}\text{Sn}_{0.4}\text{S}_{5.7}\text{Se}_{0.3}$

To induce bulk superconductivity and to increase  $T_c$ , in-plane chemical pressure effects (by chemical substitution or high-pressure annealing) are essential in the two-layer-type  $\text{BiCh}_2$ -based systems [27,28,81–83]. For example, in  $\text{LnO}_{0.5}\text{F}_{0.5}\text{BiS}_2$ , lattice shrinkage by RE site substitution in blocking layers or Se substitution for the S site in conducting layers achieve generation of in-plane chemical pressure effect and induce bulk superconductivity. We had applied the same strategy to improve superconducting properties of four-layers-type  $\text{La}_2\text{O}_2\text{Bi}_3\text{Ag}_{0.6}\text{Sn}_{0.4}\text{S}_6$  as well. Small amount (5%) of Se was substituted for the S site.  $T_c$  increased by Se substitution in  $\text{La}_2\text{O}_2\text{Bi}_3\text{Ag}_{0.6}\text{Sn}_{0.4}\text{S}_{5.7}\text{Se}_{0.3}$  [73].

A large shielding volume fraction was observed as shown in Figure 11a, which suggested the emergence of bulk superconductivity in  $\text{La}_2\text{O}_2\text{Bi}_3\text{Ag}_{0.6}\text{Sn}_{0.4}\text{S}_{5.7}\text{Se}_{0.3}$ . As we discussed above, the Sn substitution improved the superconducting properties of  $\text{La}_2\text{O}_2\text{Bi}_3\text{Ag}_{1-x}\text{Sn}_x\text{S}_6$ , and the highest  $T_c$  of 2.5 K was observed for  $x = 0.4$ . However, the shielding volume fraction for  $x = 0.4$  was clearly lower than 100% shielding. We have discussed the possible origin of an increase in  $T_c$  by Sn substitution. It was clear from the structural analysis that the essential parameter in-plane chemical pressure was not sufficient in  $\text{La}_2\text{O}_2\text{Bi}_3\text{Ag}_{0.6}\text{Sn}_{0.4}\text{S}_6$ . Since the shielding property has been improved by Se substitution, we consider that partial Se substitution for the S site in  $\text{La}_2\text{O}_2\text{Bi}_3\text{Ag}_{0.6}\text{Sn}_{0.4}\text{S}_{5.7}\text{Se}_{0.3}$  generated in-plane chemical pressure effects as observed in two-layer-type  $\text{LnO}_{0.5}\text{F}_{0.5}\text{BiS}_2$ .



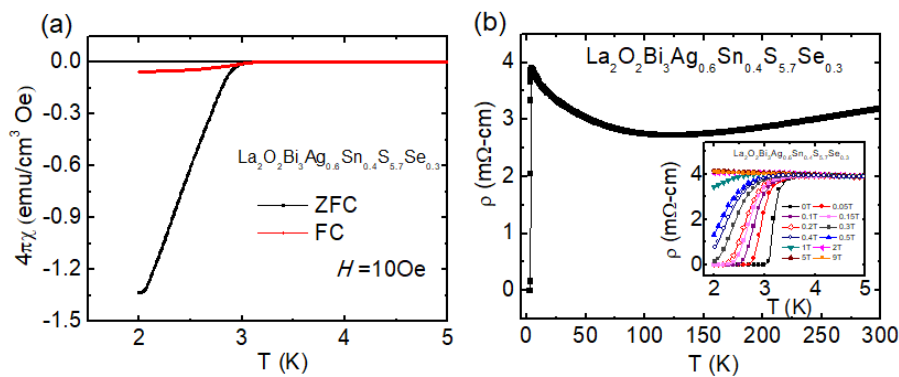
**Figure 10.** (a) Temperature ( $T$ ) dependences of magnetic susceptibility ( $\chi$ ) for  $\text{La}_2\text{O}_2\text{Bi}_3\text{Ag}_{1-x}\text{Sn}_x\text{S}_6$  ( $x = 0.3, 0.4$ , and  $0.5$ ) compounds measured in Zero Field Cool (ZFC) and Field Cool (FC) protocol at the applied magnetic field 1 mT. (b) The  $\rho(T)$  from 300–0.1 K for the  $\text{La}_2\text{O}_2\text{Bi}_3\text{Ag}_{1-x}\text{Sn}_x\text{S}_6$  ( $x = 0–0.5$ ) compounds. (c) The  $\rho(T)$  curve in the temperature range 4.0–0.1 K. (d) The  $x$  dependence of  $T_c$  for  $\text{La}_2\text{O}_2\text{Bi}_3\text{Ag}_{1-x}\text{Sn}_x\text{S}_6$  ( $x = 0–0.5$ ) compounds and  $T^*$  scaled on the  $x$ - $T$  phase diagram for  $\text{La}_2\text{O}_2\text{Bi}_3\text{Ag}_{1-x}\text{Sn}_x\text{S}_6$ . Reproduced from Sci. Rep. 9, 13346 (2019) [73], copyrighted by the Springer Nature Limited.

Figure 11b shows the temperature dependence of resistivity. Superconductivity at  $T_c$  (zero) = 3.0 K in  $\text{La}_2\text{O}_2\text{Bi}_3\text{Ag}_{0.6}\text{Sn}_{0.4}\text{S}_{5.7}\text{Se}_{0.3}$  has been confirmed by  $\rho(T)$  measurements, while the  $T_c$  (onset) was 3.5 K. From resistivity measurements under magnetic fields up to 9 T, the upper critical field  $B_{c2}$  and the irreversible field  $B_{irr}$  were estimated as 2.15 T and 1.0 T, respectively.

### 3.3.4. Eu-Substitution Effect on $\text{La}_{2-x}\text{Eu}_x\text{O}_2\text{Bi}_3\text{Ag}_{0.6}\text{Sn}_{0.4}\text{S}_6$

Since Se substitution was effective to induce bulk superconductivity in  $\text{La}_2\text{O}_2\text{Bi}_3\text{Ag}_{0.6}\text{Sn}_{0.4}\text{S}_{5.7}\text{Se}_{0.3}$ , we have tested another way to increase in-plane chemical pressure by La-site substitution by RE elements smaller than La. The first investigation was examined with RE = Eu [74]. The Sn amount was fixed as  $\text{La}_2\text{O}_2\text{Bi}_3\text{Ag}_{0.6}\text{Sn}_{0.4}\text{S}_6$ . With increasing Eu concentration,  $T_c$  increased, and the highest  $T_c$  (zero) of 4.0 K was observed for the  $x = 0.4$  (Eu), which has been confirmed by the  $\chi(T)$  and  $\rho(T)$  measurements (see Figure 12a,b). Figure 12c represents the phase diagram on  $T_c$  vs.  $x$  in  $\text{La}_{2-x}\text{Eu}_x\text{O}_2\text{Bi}_3\text{Ag}_{0.6}\text{Sn}_{0.4}\text{S}_6$ .  $T_c$  (zero)

extracted by  $\rho(T)$  data and  $T_c$  from  $\chi(T)$  curve has been plotted with Eu concentration  $x$  in Figure 12c.  $T_c$  gradually increases with increasing Eu concentration up to  $x = 0.4$  in  $\text{La}_{2-x}\text{Eu}_x\text{O}_2\text{Bi}_3\text{Ag}_{0.6}\text{Sn}_{0.4}\text{S}_6$ . Furthermore, for a higher Eu contents,  $x = 0.5$  and  $0.6$ ,  $T_c$  slightly decreased in the  $\rho(T)$  data, while  $T_c$  slightly increased for the same in  $\chi(T)$  data. The small shielding volume fraction for  $x = 0.5$  and  $0.6$  suggests that bulk nature of superconductivity was suppressed for  $x = 0.5$  and  $0.6$ . The upper critical field was estimated from  $\rho(T, B)$  data, which was above the 3.0 T for the  $\text{La}_{2-x}\text{Eu}_x\text{O}_2\text{Bi}_3\text{Ag}_{0.6}\text{Sn}_{0.4}\text{S}_6$  ( $x = 0.4$ ) confirmed the robustness of the superconductivity against the magnetic field.



**Figure 11.** (a) Temperature dependence of magnetic susceptibility for  $\text{La}_2\text{O}_2\text{Bi}_3\text{Ag}_{0.6}\text{Sn}_{0.4}\text{S}_{5.7}\text{Se}_{0.3}$ . (b) The  $\rho(T)$  for  $\text{La}_2\text{O}_2\text{Bi}_3\text{Ag}_{0.6}\text{Sn}_{0.4}\text{S}_{5.7}\text{Se}_{0.3}$ , the inset low-temperature ( $T$ ) under magnetic fields up to 9 T. Reproduced from Sci. Rep. 9, 13346 (2019) [73], copyrighted by the Springer Nature Limited.

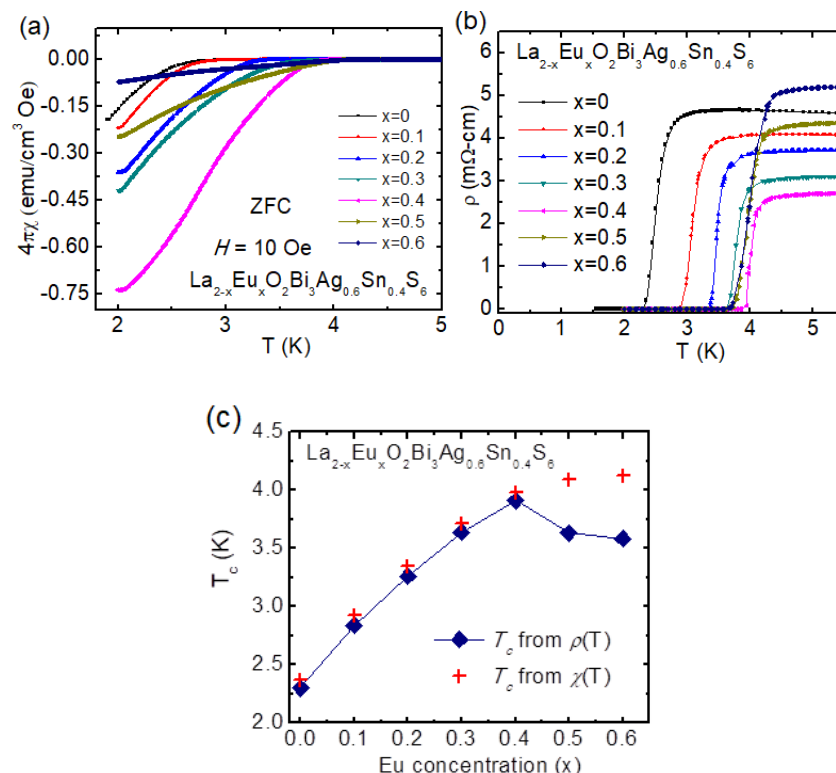


**Figure 12.** (a) The  $\chi(T)$  for  $\text{La}_{2-x}\text{Eu}_x\text{O}_2\text{Bi}_3\text{Ag}_{0.6}\text{Sn}_{0.4}\text{S}_6$  ( $x = 0-0.6$ ) for an applied magnetic field of 1 mT, compounds measured in the ZFC. (b) The  $\rho(T)$  curve is near to the  $T_c$ ; the temperature range from 5.5 K to 1.5 K for the  $\text{La}_{2-x}\text{Eu}_x\text{O}_2\text{Bi}_3\text{Ag}_{0.6}\text{Sn}_{0.4}\text{S}_6$  ( $x = 0-0.6$ ) compounds. (c) The phase diagram,  $x$  dependence of  $T_c$  for  $\text{La}_{2-x}\text{Eu}_x\text{O}_2\text{Bi}_3\text{Ag}_{0.6}\text{Sn}_{0.4}\text{S}_6$  compounds and  $T_c$  obtained from  $\chi(T)$  data,  $T_c$  obtained from  $\rho(T)$  data [74].

The increase in  $T_c$  by Eu substitution can be basically understood by the in-plane chemical pressure effect. The valence state of Eu in  $\text{La}_{2-x}\text{Eu}_x\text{O}_2\text{Bi}_3\text{Ag}_{0.6}\text{Sn}_{0.4}\text{S}_6$  is close to +3, which was analyzed from the temperature dependence of magnetic susceptibility. Since  $\text{Eu}^{3+}$  is smaller than  $\text{La}^{3+}$ , lattice should be compressed with increasing Eu concentration. As a fact, lattice parameter  $a$  decreased by Eu substitution. According to the  $a$ -axis shrinkage, in-plane chemical pressure should be enhanced in the Bi-S plane.

### 3.3.5. Rare Earth (RE) Substitution Effects in $\text{La}_{1.6}\text{RE}_{0.4}\text{O}_2\text{Bi}_3\text{Ag}_{0.6}\text{Sn}_{0.4}\text{S}_6$

In the Eu-doped  $\text{La}_{2-x}\text{Eu}_x\text{O}_2\text{Bi}_3\text{Ag}_{0.6}\text{Sn}_{0.4}\text{S}_6$ , the superconducting properties were optimized for  $x = 0.4$ . Therefore, to investigate the effects of substitution of other RE for the La site, we have synthesized samples of  $\text{La}_{2-x}\text{RE}_x\text{O}_2\text{Bi}_3\text{Ag}_{0.6}\text{Sn}_{0.4}\text{S}_6$  with  $\text{RE} = \text{Y}, \text{Pr}, \text{Nd}, \text{Sm}, \text{and Gd}$ . The XRD patterns for  $\text{La}_{1.6}\text{RE}_{0.4}\text{O}_2\text{Bi}_3\text{Ag}_{0.6}\text{Sn}_{0.4}\text{S}_6$  ( $\text{RE} = \text{Y}, \text{Pr}, \text{Nd}, \text{Sm}, \text{Eu}, \text{and Gd}$ ) are shown in Figure 13. All the XRD patterns were indexed using a tetragonal model with the space group of  $P4/nmm$ . The lattice parameter  $a$  decreases by RE doping, according to the difference in ionic radii of doped RE.

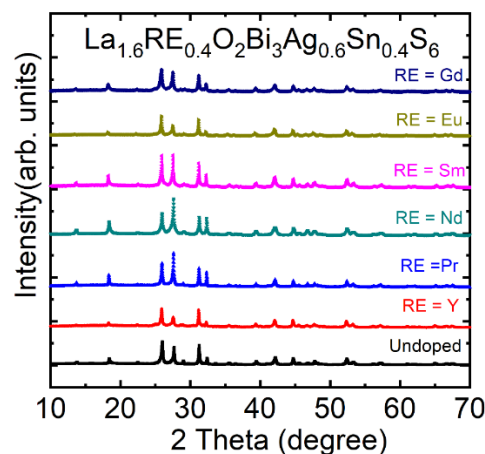


**Figure 13.** (color online) The room temperature XRD pattern of the  $\text{La}_{1.6}\text{RE}_{0.4}\text{O}_2\text{Bi}_3\text{Ag}_{0.6}\text{Sn}_{0.4}\text{S}_6$  ( $\text{RE} = \text{Y}, \text{Pr}, \text{Nd}, \text{Sm}, \text{Eu}, \text{and Gd}$ ) compounds [74].

The temperature dependence of electrical resistivity data for  $\text{La}_{1.6}\text{RE}_{0.4}\text{O}_2\text{Bi}_3\text{Ag}_{0.6}\text{Sn}_{0.4}\text{S}_6$  ( $\text{RE} = \text{Y}, \text{Pr}, \text{Nd}, \text{Sm}, \text{Eu}, \text{and Gd}$ ) has been shown in Figure 14a. The normal state resistivity shows similar behavior for all the samples, as discussed above for the Eu-doped samples. A clear difference in  $T_c$  was observed for those samples, as shown in Figure 14b. Our structural analyses for the RE-doped sample suggest that the lattice parameter  $a$  is shrinking for all the RE-doped samples. The lattice parameter  $a$  is the smallest for the Sm-doped sample, which shows the highest  $T_c = 4.1$  K.

The  $T_c$  is higher for the samples having the smallest lattice parameter  $a$ , which suggests in-plane chemical pressure is essential for  $T_c$  in  $\text{La}_{1.6}\text{RE}_{0.4}\text{O}_2\text{Bi}_3\text{Ag}_{0.6}\text{Sn}_{0.4}\text{S}_6$ . As shown in Figure 15,  $T_c$  shows a correlation with lattice parameter.  $T_c$  increases with decreasing lattice parameter  $a$ , which is suggesting in-plane chemical pressure can improve superconducting properties of  $\text{La}_{1.6}\text{RE}_{0.4}\text{O}_2\text{Bi}_3\text{Ag}_{0.6}\text{Sn}_{0.4}\text{S}_6$ , which is a common feature with two-layer-type  $\text{REO}_{0.5}\text{F}_{0.5}\text{BiCh}_2$  superconductor [22,69]. Recently, enhanced superconductivity in the Nd- and Pr-doped  $\text{La}_{2-x}\text{RE}_x\text{O}_2\text{Bi}_3\text{Ag}_{0.6}\text{Sn}_{0.4}\text{S}_6$  system has been reported in Reference 75. In the work,  $T_c$  increased for the 50%-Nd and 50%-Pr doping for the La site. The lattice parameter decreased by the Nd and Pr doping [75], which is consistent with our results.

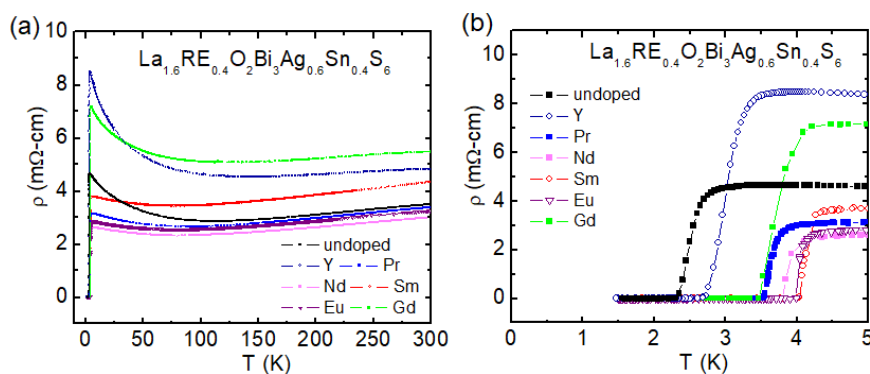


**Figure 14.** (color online) (a) The  $\rho(T)$  from 300–1.5 K for the  $\text{La}_{1.6}\text{RE}_{0.4}\text{O}_2\text{Bi}_3\text{Ag}_{0.6}\text{Sn}_{0.4}\text{S}_6$  ( $\text{RE} = \text{Y}, \text{Pr}, \text{Nd}, \text{Sm}, \text{Eu},$  and  $\text{Gd}$ ) compounds. (b) The  $\rho(T)$  from 5.0–1.5 K for the  $\text{La}_{1.6}\text{RE}_{0.4}\text{O}_2\text{Bi}_3\text{Ag}_{0.6}\text{Sn}_{0.4}\text{S}_6$  compounds [74].

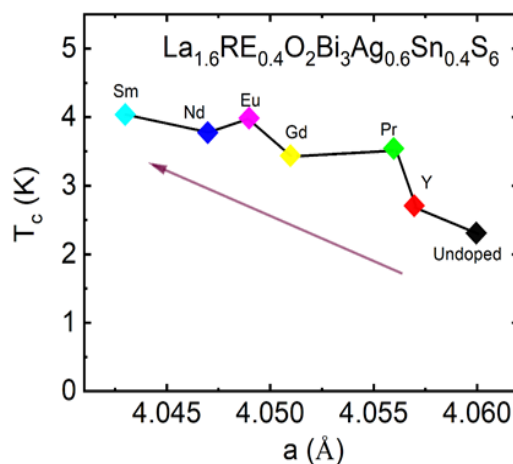


**Figure 15.** The lattice parameter  $a$  (Å) dependence of  $T_c$  for  $\text{La}_{1.6}\text{RE}_{0.4}\text{O}_2\text{Bi}_3\text{Ag}_{0.6}\text{Sn}_{0.4}\text{S}_6$  ( $\text{RE} = \text{Y}, \text{Pr}, \text{Nd}, \text{Eu}, \text{Sm},$  and  $\text{Gd}$ ) obtained from  $\rho(T)$  data [74].

There are limited studies on the theoretical investigation of  $\text{La}_2\text{O}_2\text{M}_4\text{S}_6$ -type compounds; only a few have been executed for  $\text{La}_2\text{O}_2(\text{M}_2\text{Ch}_2)(\text{Pn}_2\text{Ch}_4)$  where  $M = \text{Sn}, \text{Pb}, \text{Pn} = \text{Sb}, \text{Bi},$  and  $\text{Ch} = \text{S}, \text{Se}$  [51,84]. They suggested that a band structure could be changed by substitutions at the  $M, \text{Pn},$  and  $\text{Ch}$  sites. No one has reported about the change in electronic states by the  $\text{RE}$ -site substitution. Based on previous theoretical studies for two-layer-type  $\text{LnO}_{1-x}\text{F}_x\text{BiS}_2$  systems, we can assume that the  $\text{RE}$  substitution does not largely influence the band structure for  $\text{La}_{2-x}\text{RE}_x\text{O}_2\text{Bi}_3\text{Ag}_{0.6}\text{Sn}_{0.4}\text{S}_6$  systems. As a result that theoretical studies for  $\text{LnO}_{1-x}\text{F}_x\text{BiS}_2$  suggested that, the carrier density at the Fermi level could change slightly by changing  $\text{Ln} = \text{RE}$  in the block layers [85].

Our recent research on the four-layer-type compounds was focused to enhance the  $T_c$  at least above the 10 K, which has not been achievements yet. The maximum  $T_c$  is 4.1 K for the four-layer-type compounds. The applications of these compounds are not identified yet, as we have seen for hybrid superconducting-ferromagnetic thin films [86–88]. The study of superconducting and ferromagnetic states is important to understand the interacting mechanism of Cooper pairs and ferromagnetism [86–88], also hybrid superconducting-ferromagnetic systems are useful for the applications like; split-ring resonators, superconducting-spintronic devices, topological quantum computing, and magnetic-field-sensors as discussed in the reference [88]. There are many challenges to developing devices for the application purpose from the four-layer-type compounds.

#### 4. Summary

In this review article, we have summarized the crystal structure and physical properties of the four-layer-type  $\text{La}_2\text{O}_2\text{M}_4\text{S}_6$  system. The  $\text{La}_2\text{O}_2\text{M}_4\text{S}_6$  phase was synthesized in 2014 with  $M = \text{Bi}_2\text{Pb}_2$  by Sun et al. In 2018, superconductivity was observed in  $\text{La}_2\text{O}_2\text{Bi}_3\text{AgS}_6$ , where  $M = \text{Bi}_3\text{Ag}$ , and  $T_c$  increased up to 4.1 K by element substitution in the  $\text{La}_2\text{O}_2\text{Bi}_3\text{AgS}_6$ -based systems. The in-plane chemical pressure effects seem to be essential for the emergence of bulk superconductivity and improvement of superconducting properties in the  $\text{La}_2\text{O}_2\text{M}_4\text{S}_6$  system, which is common feature with the two-layer-type  $\text{BiCh}_2$ -based systems.

$\text{La}_2\text{O}_2\text{Bi}_2\text{Pb}_2\text{S}_6$  ( $M = \text{Bi}_2\text{Pb}_2$ ) is the firstly-synthesized  $\text{La}_2\text{O}_2\text{M}_4\text{S}_6$ -type compounds and has been reported as a thermoelectric material. The crystal structure of  $\text{La}_2\text{O}_2\text{Bi}_2\text{Pb}_2\text{S}_6$  is composed of the stacks of a  $\text{La}_2\text{O}_2\text{Bi}_2\text{S}_4$  block and a rock-salt-type  $\text{Pb}_2\text{S}_2$  layer. Thus, we can design new four-layer-type  $\text{La}_2\text{O}_2\text{M}_4\text{S}_6$  compounds by tuning the composition of the  $M_2\text{S}_2$  layer. Although  $\text{La}_2\text{O}_2\text{Bi}_2\text{Pb}_2\text{S}_6$  shows insulating behavior at low temperatures, the electrical conductivity (metallicity) has been improved by Se substitution for the  $\text{La}_2\text{O}_2\text{Bi}_2\text{Pb}_2\text{S}_6$  compound. Superconductivity has been observed for Se-doped  $\text{La}_2\text{O}_2\text{Bi}_2\text{Pb}_2\text{S}_{6-x}\text{Se}_x$ . The highest  $T_c$  was 1.9 K for  $\text{La}_2\text{O}_2\text{Bi}_2\text{Pb}_2\text{S}_{6-x}\text{Se}_x$  ( $x = 1.0$ ).

$\text{La}_2\text{O}_2\text{Bi}_3\text{AgS}_6$  ( $M = \text{Bi}_3\text{Ag}$ ) was synthesized according to the material-design strategy of  $\text{La}_2\text{O}_2\text{M}_4\text{S}_6$ .  $\text{La}_2\text{O}_2\text{Bi}_3\text{AgS}_6$  shows metallic conductivity, which is in contrast to the case of  $\text{La}_2\text{O}_2\text{Bi}_2\text{Pb}_2\text{S}_6$ .  $\text{La}_2\text{O}_2\text{Bi}_3\text{AgS}_6$  shows superconductivity at  $T_c$  (zero) = 0.5 K.  $T_c$  slightly decreased by In doping at the Ag site for  $\text{La}_2\text{O}_2\text{Bi}_3\text{Ag}_{1-x}\text{In}_x\text{S}_6$ . In contrast,  $T_c$  increased by Sn doping at the Ag site; the maximum  $T_c$  was 2.5 K for  $\text{La}_2\text{O}_2\text{Bi}_3\text{Ag}_{0.6}\text{Sn}_{0.4}\text{S}_6$ . Since the in-plane chemical pressure effect worked positively for the two-layer-type  $\text{BiCh}_2$ -based  $\text{REO}_{0.5}\text{F}_{0.5}\text{BiS}_2$  compounds, a similar approach was applied for the four-layer-type  $\text{La}_2\text{O}_2\text{M}_4\text{S}_6$  systems. Bulk superconductivity with an enhanced  $T_c$  has been obtained for the Se-doped  $\text{La}_2\text{O}_2\text{Bi}_3\text{Ag}_{0.6}\text{Sn}_{0.4}\text{S}_{5.7}\text{Se}_{0.3}$ . By Se doping at the S site in  $\text{La}_2\text{O}_2\text{Bi}_3\text{Ag}_{0.6}\text{Sn}_{0.4}\text{S}_{5.7}\text{Se}_{0.3}$ , in-plane chemical pressure was generated, which enhanced the superconducting properties of the  $\text{La}_2\text{O}_2\text{Bi}_3\text{Ag}_{0.6}\text{Sn}_{0.4}\text{S}_{5.7}\text{Se}_{0.3}$  system. In addition,  $T_c$  increased by RE-site substitution in  $\text{La}_{2-x}\text{RE}_x\text{O}_2\text{Bi}_3\text{Ag}_{0.6}\text{Sn}_{0.4}\text{S}_6$ . The effects of the RE-site substitution can be regarded as in-plane chemical pressure effects as well as the case of Se substitution. The highest  $T_c$  of 4.1 K was observed for  $x = 0.4$  in  $\text{La}_{2-x}\text{Sm}_x\text{O}_2\text{Bi}_3\text{Ag}_{0.6}\text{Sn}_{0.4}\text{S}_6$ . Bulk nature of superconductivity has been confirmed by magnetic susceptibility measurements, and the corresponding shielding volume fraction exceeded 75% for  $x = 0.4$  for the Eu- and Sm-doped systems. The structural analysis suggested the solubility limit of RE in the  $\text{La}_{2-x}\text{RE}_x\text{O}_2\text{Bi}_3\text{Ag}_{0.6}\text{Sn}_{0.4}\text{S}_6$  system is  $x \sim 0.4$ , at which the high  $T_c$  was observed. In  $\text{La}_{2-x}\text{RE}_x\text{O}_2\text{Bi}_3\text{Ag}_{0.6}\text{Sn}_{0.4}\text{S}_6$ , the lattice parameter  $a$  and  $T_c$  showed good correlation, which is suggesting the importance of in-plane chemical pressure. Our review article may enhance the visibility of four-layer-type  $\text{La}_2\text{O}_2\text{M}_4\text{S}_6$  systems, which should be necessary for further development of Bi-based layered superconductors.

#### 5. Experimental Details

We are showing new data for the  $\text{La}_2\text{O}_2\text{Bi}_2\text{Pb}_{2-x}\text{Cd}_x\text{S}_6$ ,  $\text{La}_2\text{O}_2\text{Bi}_2\text{Pb}_{2-x}\text{Sn}_x\text{S}_6$ , and  $\text{La}_2\text{O}_2\text{Bi}_2\text{Pb}_{2-x}\text{Sb}_x\text{S}_6$  samples. The polycrystalline samples of  $\text{La}_2\text{O}_2\text{Bi}_2\text{Pb}_{2-x}\text{Cd}_x\text{S}_6$ ,  $\text{La}_2\text{O}_2\text{Bi}_2\text{Pb}_{2-x}\text{Sn}_x\text{S}_6$ , and  $\text{La}_2\text{O}_2\text{Bi}_2\text{Pb}_{2-x}\text{Sb}_x\text{S}_6$  were synthesized by a solid-state reaction method. Powders of  $\text{La}_2\text{S}_3$  (99.99%),  $\text{Bi}_2\text{O}_3$  (99.9%), Pb (99.99%), Cd (99.99%), Sn (99.99%), Sb (99.99%), and grains of Bi (99.999%), S (99.99%) with a nominal composition were mixed in a pestle and mortar, pelletized, sealed in an evacuated quartz tube, and heated at 720 °C for 15 h. For the homogeneity the samples were reground, pelletized, and heated at 720 °C for 15 h. The phase purity has been checked by X-ray diffraction (XRD) with Cu-K $\alpha$  radiation. The crystal structure parameters were refined by using the Rietveld method with RIETAN-FP [89]. The schematic images of the crystal structure were drawn using VESTA [90]. The actual compositions of the synthesized samples were investigated by using energy-dispersive X-ray spectroscopy (EDX) with TM-3030 (Hitachi). The electrical resistivity down to  $T = 2.0$  K was measured by the four-probe technique. The temperature dependence of magnetic susceptibility  $\chi$

(T) was measured by using a superconducting quantum interference device (SQUID) magnetometer (MPMS-3, Quantum Design).

**Author Contributions:** R.J. and Y.M.; writing—original draft preparation, R.J. and Y.M.; writing—review and editing, R.J. and Y.M.; visualization, Y.M.; supervision, Y.M.; project administration, Y.M.; funding acquisition, Y.M. All authors have read and agreed to the published version of the manuscript.

**Funding:** This work was financially supported by Grants in Aid for Scientific Research (KAKENHI) (Grant No. 15H05886) and the Advanced Research Program under the Human Resources Funds of Tokyo (Grant Number: H31-1).

**Acknowledgments:** We gratefully appreciate O. Miura, Y. Goto, R. Higashinaka, T. D. Matsuda, and Y. Aoki of Tokyo Metropolitan University for fruitful discussions.

**Conflicts of Interest:** The authors declare no conflict of interest.

## References

1. Bednorz, J.G.; Muller, K.A. Possible high  $T_c$  superconductivity in the Ba–La–Cu–O system. *Z. Phys. B* **1986**, *64*, 189–193. [[CrossRef](#)]
2. Kamihara, Y.; Watanabe, T.; Hirano, M.; Hosono, H. Iron-Based Layered Superconductor  $\text{La}[\text{O}_{1-x}\text{F}_x]\text{FeAs}$  ( $x = 0.05\text{--}0.12$ ) with  $T_c = 26$  K. *J. Am. Chem. Soc.* **2008**, *130*, 3296–3297. [[CrossRef](#)] [[PubMed](#)]
3. Mizuguchi, Y.; Fujihisa, H.; Gotoh, Y.; Suzuki, K.; Usui, H.; Kuroki, K.; Demura, S.; Takano, Y.; Izawa, H.; Miura, O.  $\text{BiS}_2$ -based layered superconductor  $\text{Bi}_4\text{O}_4\text{S}_3$ . *Phys. Rev. B* **2012**, *86*, 220510. [[CrossRef](#)]
4. Mizuguchi, Y.; Demura, S.; Deguchi, K.; Takano, Y.; Fujihisa, H.; Gotoh, Y.; Izawa, H.; Miura, O. Superconductivity in Novel  $\text{BiS}_2$ -Based Layered Superconductor  $\text{LaO}_{1-x}\text{F}_x\text{BiS}_2$ . *J. Phys. Soc. Jpn.* **2012**, *81*, 114725. [[CrossRef](#)]
5. Singh, S.K.; Kumar, A.; Gahtori, B.; Kirtan, S.; Sharma, G.; Patnaik, S.; Awana, V.P.S. Bulk Superconductivity in Bismuth Oxysulfide  $\text{Bi}_4\text{O}_4\text{S}_3$ . *J. Am. Chem. Soc.* **2012**, *134*, 16504–16507. [[CrossRef](#)] [[PubMed](#)]
6. Demura, S.; Mizuguchi, Y.; Deguchi, K.; Okazaki, H.; Hara, H.; Watanabe, T.; Denholme, S.J.; Fujioka, M.; Ozaki, T.; Fujihisa, H.; et al. New Member of  $\text{BiS}_2$ -Based Superconductor  $\text{NdO}_{1-x}\text{F}_x\text{BiS}_2$ . *J. Phys. Soc. Jpn.* **2013**, *82*, 033708. [[CrossRef](#)]
7. Jha, R.; Kumar, A.; Singh, S.K.; Awana, V.P.S. Superconductivity at 5 K in  $\text{NdO}_{0.5}\text{F}_{0.5}\text{BiS}_2$ . *J. Appl. Phys.* **2013**, *113*, 056102. [[CrossRef](#)]
8. Jha, R.; Kumar, A.; Singh, S.K.; Awana, V.P.S. Synthesis and Superconductivity of New  $\text{BiS}_2$ -Based Superconductor  $\text{PrO}_{0.5}\text{F}_{0.5}\text{BiS}_2$ . *J. Supercond. Nov. Magn.* **2013**, *26*, 499–502. [[CrossRef](#)]
9. Xing, J.; Li, S.; Ding, X.; Yang, H.; Wen, H.H. Superconductivity appears in the vicinity of semiconducting-like behavior in  $\text{CeO}_{1-x}\text{F}_x\text{BiS}_2$ . *Phys. Rev. B* **2012**, *86*, 214518. [[CrossRef](#)]
10. Yazici, D.; Huang, K.; White, B.D.; Chang, A.H.; Friedman, A.J.; Maple, M.B. Superconductivity of F-substituted  $\text{LnOBiS}_2$  ( $\text{Ln}=\text{La, Ce, Pr, Nd, Yb}$ ) compounds. *Philos. Mag.* **2012**, *93*, 673–680. [[CrossRef](#)]
11. Yazici, D.; Huang, K.; White, B.D.; Jeon, I.; Burnett, V.W.; Friedman, A.J.; Lum, I.K.; Nallaiyan, M.; Spagna, S.; Maple, M.B. Superconductivity induced by electron doping in  $\text{La}_{1-x}\text{MxOBiS}_2$  ( $\text{M}=\text{Ti, Zr, Hf, Th}$ ). *Phys. Rev. B* **2013**, *87*, 174512. [[CrossRef](#)]
12. Krzton-Maziopa, A.; Guguchia, Z.; Pomjakushina, E.; Pomjakushin, V.; Khasanov, R.; Luetkens, H.; Biswas, P.; Amato, A.; Keller, H.; Conder, K. Superconductivity in a new layered bismuth oxyselenide:  $\text{LaO}_{0.5}\text{F}_{0.5}\text{BiSe}_2$ . *J. Phys.-Condens. Matter* **2014**, *26*, 215702. [[CrossRef](#)] [[PubMed](#)]
13. Mizuguchi, Y.; Omachi, A.; Goto, Y.; Kamihara, Y.; Matoba, M.; Hiroi, T.; Kajitani, J.; Miura, O. Enhancement of thermoelectric properties by Se substitution in layered bismuth-chalcogenide  $\text{LaOBiS}_{2-x}\text{Se}_x$ . *J. Appl. Phys.* **2014**, *116*, 163915. [[CrossRef](#)]
14. Lin, X.; Ni, X.; Chen, B.; Xu, X.; Yang, X.; Dai, J.; Li, Y.; Yang, X.; Luo, Y.; Tao, Q.; et al. Superconductivity induced by La doping in  $\text{Sr}_{1-x}\text{La}_x\text{FBiS}_2$ . *Phys. Rev. B* **2013**, *87*, 020504. [[CrossRef](#)]
15. Zhai, H.F.; Tang, Z.T.; Jiang, H.; Xu, K.; Zhang, K.; Zhang, P.; Bao, J.K.; Sun, Y.L.; Jiao, W.H.; Nowik, I.; et al. Possible charge-density wave, superconductivity, and f-electron valence instability in  $\text{EuBiS}_2\text{F}$ . *Phys. Rev. B* **2014**, *90*, 064518. [[CrossRef](#)]
16. Kotegawa, H.; Tomita, Y.; Tou, H.; Izawa, H.; Mizuguchi, Y.; Miura, O.; Demura, S.; Deguchi, K.; Takano, Y. Pressure Study of  $\text{BiS}_2$ -Based Superconductors  $\text{Bi}_4\text{O}_4\text{S}_3$  and  $\text{La}(\text{O,F})\text{BiS}_2$ . *J. Phys. Soc. Jpn.* **2012**, *81*, 103702. [[CrossRef](#)]

17. Wolowiec, C.T.; Yazici, D.; White, B.D.; Huang, K.; Maple, M.B. Pressure-induced enhancement of superconductivity and suppression of semiconducting behavior in  $LnO_{0.5}F_{0.5}BiS_2$  ( $Ln=La,Ce$ ) compounds. *Phys. Rev. B* **2013**, *88*, 064503. [[CrossRef](#)]
18. Wolowiec, C.T.; White, B.D.; Jeon, I.; Yazici, D.; Huang, K.; Maple, M.B. Enhancement of superconductivity near the pressure-induced semiconductor–metal transition in the  $BiS_2$ -based superconductors  $LnO_{0.5}F_{0.5}BiS_2$  ( $Ln = La, Ce, Pr, Nd$ ). *J. Phys. Condens. Matter* **2013**, *25*, 422201. [[CrossRef](#)]
19. Jha, R.; Tiwari, B.; Awana, V.P.S. Impact of Hydrostatic Pressure on Superconductivity of  $Sr_{0.5}La_{0.5}FBiS_2$ . *J. Phys. Soc. Jpn.* **2014**, *83*, 063707. [[CrossRef](#)]
20. Jha, R.; Tiwari, B.; Awana, V.P.S. Appearance of bulk superconductivity under hydrostatic pressure in  $Sr_{0.5}RE_{0.5}FBiS_2$  ( $RE = Ce, Nd, Pr, \text{ and } Sm$ ) compounds. *J. Appl. Phys.* **2015**, *117*, 013901. [[CrossRef](#)]
21. Mizuguchi, Y.; Miura, A.; Kajitani, J.; Hiroi, T.; Miura, O.; Tadanaga, K.; Kumada, N.; Magome, E.; Moriyoshi, C.; Kuroiwa, Y. In-plane chemical pressure essential for superconductivity in  $BiCh_2$ -based ( $Ch: S, Se$ ) layered structure. *Sci. Rep.* **2015**, *5*, 14968. [[CrossRef](#)] [[PubMed](#)]
22. Kajitani, J.; Hiroi, T.; Omachi, A.; Miura, O.; Mizuguchi, Y. Chemical Pressure Effect on Superconductivity of  $BiS_2$ -Based  $Ce_{1-x}Nd_xO_{1-y}F_yBiS_2$  and  $Nd_{1-z}Sm_zO_{1-y}F_yBiS_2$ . *J. Phys. Soc. Jpn.* **2015**, *84*, 044712. [[CrossRef](#)]
23. Paris, E.; Joseph, B.; Iadecola, A.; Sugimoto, T.; Olivi, L.; Demura, S.; Mizuguchi, Y.; Takano, Y.; Mizokawa, T.; Saini, N.L. Determination of local atomic displacements in  $CeO_{1-x}F_xBiS_2$  system. *J. Phys. Condens. Matter* **2014**, *26*, 435701.
24. Mizuguchi, Y.; Paris, E.; Sugimoto, T.; Iadecola, A.; Kajitani, J.; Miura, O.; Mizokawa, T.; Saini, N.L. The effect of RE substitution in layered  $REO_{0.5}F_{0.5}BiS_2$ : Chemical pressure, local disorder and superconductivity. *Phys. Chem. Chem. Phys.* **2015**, *17*, 22090–22096. [[CrossRef](#)] [[PubMed](#)]
25. Athauda, A.; Yang, J.; Lee, S.; Mizuguchi, Y.; Deguchi, K.; Takano, Y.; Miura, O.; Louca, D. In-plane charge fluctuations in bismuth-sulfide superconductors. *Phys. Rev. B* **2015**, *91*, 144112. [[CrossRef](#)]
26. Nagasaka, K.; Nishida, A.; Jha, R.; Kajitani, J.; Miura, O.; Higashinaka, R.; Matsuda, T.D.; Aoki, Y.; Miura, A.; Moriyoshi, C.; et al. Intrinsic Phase Diagram of Superconductivity in the  $BiCh_2$ -Based System Without In-Plane Disorder. *J. Phys. Soc. Jpn.* **2017**, *86*, 074701. [[CrossRef](#)]
27. Mizuguchi, Y. Material Development and Physical Properties of  $BiS_2$ -Based Layered Compounds. *J. Phys. Soc. Jpn.* **2019**, *88*, 041001. [[CrossRef](#)]
28. Jinno, G.; Jha, R.; Yamada, A.; Higashinaka, R.; Matsuda, T.D.; Aoki, Y.; Nagao, M.; Miura, O.; Mizuguchi, Y. Bulk Superconductivity Induced by In-Plane Chemical Pressure Effect in  $Eu_{0.5}La_{0.5}FBiS_{2-x}Sex$ . *J. Phys. Soc. Jpn.* **2016**, *85*, 124708. [[CrossRef](#)]
29. Tanaka, M.; Yamaki, T.; Matsushita, Y.; Fujioka, M.; Denholme, S.J.; Yamaguchi, T.; Takeya, H.; Takano, Y. Site selectivity on chalcogen atoms in superconducting  $La(O,F)BiS_2$ . *Appl. Phys. Lett.* **2015**, *106*, 112601. [[CrossRef](#)]
30. Hiroi, T.; Kajitani, J.; Omachi, A.; Miura, O.; Mizuguchi, Y. Evolution of Superconductivity in  $BiS_2$ -Based Superconductor  $LaO_{0.5}F_{0.5}Bi(S_{1-x}Se_x)_2$ . *J. Phys. Soc. Jpn.* **2015**, *84*, 024723. [[CrossRef](#)]
31. Tanaka, M.; Nagao, M.; Matsushita, Y.; Fujioka, M.; Denholme, S.J.; Yamaguchi, T.; Takeya, H.; Takano, Y. First single crystal growth and structural analysis of superconducting layered bismuth oxyselenide;  $La(O,F)BiSe_2$ . *J. Solid State Chem.* **2014**, *219*, 168. [[CrossRef](#)]
32. Nagao, M.; Tanaka, M.; Watauchi, S.; Tanaka, I.; Takano, Y. Superconducting Anisotropies of F-Substituted  $LaOBiSe_2$  Single Crystals. *J. Phys. Soc. Jpn.* **2014**, *83*, 114709. [[CrossRef](#)]
33. Feng, Y.; Ding, H.C.; Du, Y.; Wan, X.; Wang, B.; Savrasov, S.Y.; Duan, C.G. Electron-phonon superconductivity in  $LaO_{0.5}F_{0.5}BiSe_2$ . *J. Appl. Phys.* **2014**, *115*, 233901. [[CrossRef](#)]
34. Wang, G.; Wang, D.; Shi, X.; Peng, Y. First-principles study of the electronic structure and thermoelectric properties of  $LaOBiCh_2$  ( $Ch = S, Se$ ). *Mod. Phys. Lett. B* **2017**, *31*, 1750265. [[CrossRef](#)]
35. Liu, J.; Li, S.; Li, Y.; Zhu, X.; Wen, H.H. Pressure-tuned enhancement of superconductivity and change of ground state properties in  $LaO_{0.5}F_{0.5}BiSe_2$  single crystals. *Phys. Rev. B* **2014**, *90*, 094507. [[CrossRef](#)]
36. Shao, J.; Liu, Z.; Yao, X.; Zhang, L.; Pi, L.; Tan, S.; Zhang, C.; Zhang, Y. Superconducting properties of  $BiSe_2$ -based  $LaO_{1-x}F_xBiSe_2$  single crystals. *EPL* **2014**, *107*, 37006. [[CrossRef](#)]
37. Fujioka, M.; Tanaka, M.; Denholme, S.J.; Yamaki, T.; Takeya, H.; Yamaguchi, T.; Takano, Y. Pressure-induced phase transition for single-crystalline  $LaO_{0.5}F_{0.5}BiSe_2$ . *EPL* **2014**, *108*, 47007. [[CrossRef](#)]
38. Hoshi, K.; Goto, Y.; Mizuguchi, Y. Selenium isotope effect in the layered bismuth chalcogenide superconductor  $LaO_{0.6}F_{0.4}Bi(S,Se)_2$ . *Phys. Rev. B* **2018**, *97*, 094509. [[CrossRef](#)]



39. Jha, R.; Awana, V.P.S. Anomalous Impact of Hydrostatic Pressure on Superconductivity of Polycrystalline  $\text{LaO}_{0.5}\text{F}_{0.5}\text{BiSe}_2$ . *J. Supercond. Nov. Magn.* **2015**, *28*, 2229–2233. [[CrossRef](#)]
40. Nishida, A.; Miura, O.; Lee, C.H.; Mizuguchi, Y. High thermoelectric performance and low thermal conductivity of densified  $\text{LaOBiSSe}$ . *Appl. Phys. Express* **2015**, *8*, 111801. [[CrossRef](#)]
41. Mizuguchi, Y.; Hiroi, T.; Miura, O. Superconductivity phase diagram of Se-substituted  $\text{CeO}_{0.5}\text{F}_{0.5}\text{Bi}(\text{S}_{1-x}\text{Se}_x)_2$ . *J. Phys. Conf. Ser.* **2016**, *683*, 012001. [[CrossRef](#)]
42. Hoshi, K.; Kimata, M.; Goto, Y.; Matsuda, T.D.; Mizuguchi, Y. Two-Fold-Symmetric Magnetoresistance in Single Crystals of Tetragonal  $\text{BiCh}_2$ -Based Superconductor  $\text{LaO}_{0.5}\text{F}_{0.5}\text{BiSSe}$ . *J. Phys. Soc. Jpn.* **2019**, *88*, 033704. [[CrossRef](#)]
43. Mizuguchi, Y.; Miura, A.; Nishida, A.; Miura, O.; Tadanaga, K.; Kumada, N.; Lee, C.H.; Magome, E.; Moriyoshi, C.; Kuroiwa, Y. Compositional and temperature evolution of crystal structure of new thermoelectric compound  $\text{LaOBiS}_{2-x}\text{Se}_x$ . *J. Appl. Phys.* **2016**, *119*, 155103. [[CrossRef](#)]
44. Lee, C.H.; Nishida, A.; Hasegawa, T.; Nishiate, H.; Kunioka, H.; Ohira-Kawamura, S.; Nakamura, M.; Nakajima, K.; Mizuguchi, Y. Effect of rattling motion without cage structure on lattice thermal conductivity in  $\text{LaOBiS}_{2-x}\text{Se}_x$ . *Appl. Phys. Lett.* **2018**, *112*, 023903. [[CrossRef](#)]
45. Kase, N.; Terui, Y.; Nakano, T.; Takeda, N. Superconducting gap symmetry of the  $\text{BiS}_2$ -based superconductor  $\text{LaO}_{0.5}\text{F}_{0.5}\text{BiSSe}$  elucidated through specific heat measurements. *Phys. Rev. B* **2017**, *96*, 214506. [[CrossRef](#)]
46. Nagao, M.; Demura, S.; Deguchi, K.; Miura, A.; Watauchi, S.; Takei, T.; Takano, Y.; Kumada, N.; Tanaka, I. Structural Analysis and Superconducting Properties of F-Substituted  $\text{NdOBiS}_2$  Single Crystals. *J. Phys. Soc. Jpn.* **2013**, *82*, 113701. [[CrossRef](#)]
47. Liu, J.; Fang, D.; Wang, Z.; Xing, J.; Du, Z.; Zhu, X.; Yang, H.; Wen, H.H. Giant superconducting fluctuation and anomalous semiconducting normal state in  $\text{NdO}_{1-x}\text{F}_x\text{Bi}_{1-y}\text{S}_2$  single crystals. *EPL* **2014**, *106*, 67002. [[CrossRef](#)]
48. Nagao, M. Growth and characterization of  $\text{R}(\text{O,F})\text{BiS}_2$  ( $\text{R} = \text{La, Ce, Pr, Nd}$ ) superconducting single crystals. *Nov. Supercond. Mater.* **2015**, *1*, 64–74. [[CrossRef](#)]
49. Sun, Y.L.; Ablimit, A.; Zhai, H.F.; Bao, J.K.; Tang, Z.T.; Wang, X.B.; Wang, N.L.; Feng, C.M.; Cao, G.H. Design and Synthesis of a New Layered Thermoelectric Material  $\text{LaPbBi}_3\text{O}$ . *Inorg. Chem.* **2014**, *53*, 11125–11129. [[CrossRef](#)]
50. Mizuguchi, Y.; Hijikata, Y.; Abe, T.; Moriyoshi, C.; Kuroiwa, Y.; Goto, Y.; Miura, A.; Lee, S.; Torii, S.; Kamiyama, T.; et al. Crystal structure, site selectivity, and electronic structure of layered chalcogenide  $\text{LaOBiPbS}_3$ . *EPL* **2017**, *119*, 26002. [[CrossRef](#)]
51. Hijikata, Y.; Abe, T.; Moriyoshi, C.; Kuroiwa, Y.; Goto, Y.; Miura, A.; Tadanaga, K.; Wang, Y.; Miura, O.; Mizuguchi, Y. Synthesis, Crystal Structure, and Physical Properties of New Layered Oxychalcogenide  $\text{La}_2\text{O}_2\text{Bi}_3\text{AgS}_6$ . *J. Phys. Soc. Jpn.* **2017**, *86*, 124802. [[CrossRef](#)]
52. Jha, R.; Goto, Y.; Higashinaka, R.; Matsuda, T.D.; Aoki, Y.; Mizuguchi, Y. Superconductivity in Layered Oxychalcogenide  $\text{La}_2\text{O}_2\text{Bi}_3\text{AgS}_6$ . *J. Phys. Soc. Jpn.* **2018**, *87*, 083704. [[CrossRef](#)]
53. Wu, M.K.; Ashburn, J.R.; Torng, C.J.; Hor, P.H.; Meng, R.L.; Gao, L.; Huang, Z.J.; Wang, Y.Q.; Chu, C.W. Superconductivity at 93 K in a new mixed-phase Y-Ba-Cu-O compound system at ambient pressure. *Phys. Rev. Lett.* **1987**, *58*, 908. [[CrossRef](#)] [[PubMed](#)]
54. Cava, R.J.; Van Dover, R.B.; Batlogg, B.; Rietman, E.A. Bulk superconductivity at 36 K in  $\text{La}_{1.8}\text{Sr}_{0.2}\text{CuO}_4$ . *Phys. Rev. Lett.* **1987**, *58*, 408. [[CrossRef](#)]
55. PELIKÁN, P. The relation between structure and superconductive properties of high-temperature superconductors. *Chem. Papers* **1990**, *44*, 721–736.
56. Hazen, R.M.; Prewitt, C.T.; Angel, R.J.; Ross, N.L.; Finger, L.W.; Hadidiacos, C.G.; Veblen, D.R.; Heaney, P.J.; Hor, P.H.; Meng, R.L.; et al. Superconductivity in the high- $T_c$  Bi-Ca-Sr-Cu-O system: Phase identification. *Phys. Rev. Lett.* **1988**, *60*, 1174. [[CrossRef](#)]
57. Maeda, H.; Tanaka, Y.; Fukitoki, M.; Asano, T. A New High- $T_c$  Oxide Superconductor without a Rare Earth Element. *Jpn. J. Appl. Phys.* **1988**, *27*, L209. [[CrossRef](#)]
58. Eisaki, H.; Kaneko, N.; Feng, D.L.; Damascelli, A.; Mang, P.K.; Shen, K.M.; Shen, Z.X.; Greven, M. Effect of chemical inhomogeneity in bismuth-based copper oxide superconductors. *Phys. Rev. B* **2004**, *69*, 064512. [[CrossRef](#)]
59. Brandt, B.; Ginzburg, N.I. Critical Fields of the Crystalline Modifications Bi II and Bi III. *SoV. Phys. JETP* **1963**, *17*, 326.

60. Stromberg, H.D.; Stephens, D.R. Effects of pressure on the electrical resistance of certain metals. *J. Phys. Chem. Solids* **1964**, *25*, 1015. [[CrossRef](#)]
61. Brandt, N.B.; Ginzburg, N.I. Superconductivity at high pressures. *Comtemp. Phys.* **1969**, *10*, 355. [[CrossRef](#)]
62. Weitzel, B.; Micklitz, H. Superconductivity in granular systems built from well-defined rhombohedral Bi-clusters: Evidence for Bi-surface superconductivity. *Phys. Rev. Lett.* **1991**, *66*, 385. [[CrossRef](#)]
63. Liu, L.Y.; Xing, Y.T.; Merino, I.L.C.; Micklitz, H.; Franceschini, D.F.; Baggio-Saitovitch, E.; Bell, D.C.; Solorzano, I.G. Superconductivity in Bi/Ni bilayer system: Clear role of superconducting phases found at Bi/Ni interface. *Phys. Rev. Mater.* **2018**, *2*, 014601. [[CrossRef](#)]
64. Chao, S.P. Superconductivity in a Bi/Ni bilayer. *Phys. Rev. B* **2019**, *99*, 064504. [[CrossRef](#)]
65. Tian, M.; Wang, J.; Kumar, N.; Han, T.; Kobayashi, Y.; Liu, Y.; Mallouk, T.E.; Chan, M.H.W. Observation of Superconductivity in Granular Bi Nanowires Fabricated by Electrodeposition. *Nano Lett.* **2006**, *6*, 2773–2780. [[CrossRef](#)] [[PubMed](#)]
66. Kumar, J.; Kumar, A.; Vajpayee, A.; Gahtori, B.; Sharma, D.; Ahluwalia, P.K.; Auluck, S.; Awana, V.P.S. Physical property and electronic structure characterization of bulk superconducting Bi<sub>3</sub>Ni. *Supercond. Sci. Technol.* **2011**, *24*, 085002. [[CrossRef](#)]
67. Jha, R.; Avila, M.A.; Ribeiro, R.A. Hydrostatic pressure effect on the superconducting properties of BaBi<sub>3</sub> and SrBi<sub>3</sub> single crystals. *Supercond. Sci. Technol.* **2017**, *30*, 025015. [[CrossRef](#)]
68. Fang, Y.; Yazici, D.; White, B.D.; Maple, M.B. Enhancement of superconductivity in La<sub>1-x</sub>Sm<sub>x</sub>O<sub>0.5</sub>F<sub>0.5</sub>BiS<sub>2</sub>. *Phys. Rev. B* **2015**, *91*, 064510. [[CrossRef](#)]
69. Jeon, I.; Yazici, D.; White, B.D.; Friedman, A.J.; Maple, M.B. Effect of yttrium substitution on the superconducting properties of La<sub>1-x</sub>Y<sub>x</sub>O<sub>0.5</sub>F<sub>0.5</sub>BiS<sub>2</sub>. *Phys. Rev. B* **2014**, *90*, 054510. [[CrossRef](#)]
70. Thakur, G.S.; Selvan, G.K.; Haque, Z.; Gupta, L.C.; Samal, S.L.; Arumugam, S.; Ganguli, A.K. Synthesis and Properties of SmO<sub>0.5</sub>F<sub>0.5</sub>BiS<sub>2</sub> and Enhancement in T<sub>c</sub> in La<sub>1-y</sub>Sm<sub>y</sub>O<sub>0.5</sub>F<sub>0.5</sub>BiS<sub>2</sub>. *Inorg.Chem.* **2015**, *54*, 1076–1081. [[CrossRef](#)]
71. Mizuguchi, Y.; Hoshi, K.; Goto, Y.; Miura, A.; Tadanaga, K.; Moriyoshi, C.; Kuroiwa, Y. Evolution of Anisotropic Displacement Parameters and Superconductivity with Chemical Pressure in BiS<sub>2</sub>-Based REO<sub>0.5</sub>F<sub>0.5</sub>BiS<sub>2</sub> (RE = La, Ce, Pr, and Nd). *J. Phys. Soc. Jpn.* **2018**, *87*, 023704. [[CrossRef](#)]
72. Paris, E.; Mizuguchi, Y.; Hacisalihoglu, M.Y.; Hiroi, T.; Joseph, B.; Aquilanti, G.; Miura, O.; Mizokawa, T.; Saini, N.L. Role of the local structure in superconductivity of LaO<sub>0.5</sub>F<sub>0.5</sub>BiS<sub>2-x</sub>Se<sub>x</sub> system. *J. Phys.-Condens. Matter* **2017**, *29*, 145603. [[CrossRef](#)] [[PubMed](#)]
73. Jha, R.; Goto, Y.; Matsuda, T.D.; Aoki, Y.; Nagao, M.; Tanaka, I.; Mizuguchi, Y. Bulk superconductivity in a four-layer-type Bi-based compound La<sub>2</sub>O<sub>2</sub>Bi<sub>3</sub>Ag<sub>0.6</sub>Sn<sub>0.4</sub>S<sub>5.7</sub>Se<sub>0.3</sub>. *Sci. Rep.* **2019**, *9*, 13346. [[CrossRef](#)] [[PubMed](#)]
74. Jha, R.; Goto, Y.; Higashinaka, R.; Miura, A.; Moriyoshi, C.; Kuroiwa, Y.; Mizuguchi, Y. Improvement of superconducting properties by chemical pressure effect in Eu-doped La<sub>2-x</sub>Eu<sub>x</sub>O<sub>2</sub>Bi<sub>3</sub>Ag<sub>0.6</sub>Sn<sub>0.4</sub>S<sub>6</sub>. *arXiv* **2019**, arXiv:1908.09311.
75. Kim, G.C.; Cheon, M.; Choi, W.; Ahmad, D.; Kwon, Y.S.; Ko, R.; Kim, Y.C. Superconductivity in Oxychalcogenide LaREO<sub>2</sub>Bi<sub>3</sub>Ag<sub>0.6</sub>Sn<sub>0.4</sub>S<sub>6</sub> (RE = Pr and Nd). *J. Supercond. Nov. Magn.* **2019**, *33*, 625. [[CrossRef](#)]
76. Ruan, B.B.; Zhao, K.; Mu, Q.G.; Pan, B.J.; Liu, T.; Yang, H.X.; Li, J.Q.; Chen, G.F.; Ren, Z.A. Superconductivity in Bi<sub>3</sub>O<sub>2</sub>S<sub>2</sub>Cl with Bi-Cl Planar Layers. *J. Am. Chem. Soc.* **2019**, *141*, 3404. [[CrossRef](#)]
77. Jha, R.; Goto, Y.; Matsuda, T.D.; Aoki, Y.; Mizuguchi, Y. Superconductivity in Se-doped La<sub>2</sub>O<sub>2</sub>Bi<sub>2</sub>Pb<sub>2</sub>S<sub>6-x</sub>Se<sub>x</sub> with a Bi<sub>2</sub>Pb<sub>2</sub>Ch<sub>4</sub>-type thick conducting layer. *arXiv* **2019**, arXiv:1912.11981.
78. Jha, R.; Goto, Y.; Matsuda, T.D.; Aoki, Y.; Mizuguchi, Y. Effect of Indium doping on the superconductivity of layered oxychalcogenide La<sub>2</sub>O<sub>2</sub>Bi<sub>3</sub>Ag<sub>1-x</sub>In<sub>x</sub>S<sub>6</sub>. In *Journal of Physics: Conference Series*; IOP Publishing: Bristol, UK, 2019; Volume 1293, p. 012001.
79. Jerome, D.; Berthier, C.; Molinie, P.; Rouxel, J. Layer compounds. Charge density waves in transition metal compounds. Electronic properties of transition metal dichalcogenides: Connection between structural instabilities and superconductivity. *J. Physique Colloq.* **1976**, *37*, C4-125–C4-135.
80. Li, L.; Deng, X.; Wang, Z.; Liu, Y.; Abeykoon, M.; Dooryhee, E.; Tomic, A.; Huang, Y.; Warren, J.B.; Bozin, E.S.; et al. Superconducting order from disorder in 2H-TaSe<sub>2-x</sub>S<sub>x</sub>. *npj Quantum Mater.* **2017**, *2*, 11. [[CrossRef](#)]
81. Goto, Y.; Sogabe, R.; Mizuguchi, Y. Bulk Superconductivity Induced by Se Substitution in BiCh<sub>2</sub>-Based Layered Compounds Eu<sub>0.5</sub>Ce<sub>0.5</sub>FBiS<sub>2-x</sub>Se<sub>x</sub>. *J. Phys. Soc. Jpn.* **2017**, *86*, 104712. [[CrossRef](#)]

82. Pallecchi, I.; Lamura, G.; Putti, M.; Kajitani, J.; Mizuguchi, Y.; Miura, O.; Demura, S.; Deguchi, K.; Takano, Y. Effect of high-pressure annealing on the normal-state transport of  $\text{LaO}_{0.5}\text{F}_{0.5}\text{BiS}_2$ . *Phys. Rev. B* **2014**, *89*, 214513. [[CrossRef](#)]
83. Nishida, A.; Nishiate, H.; Lee, C.H.; Miura, O.; Mizuguchi, Y. Electronic Origins of Large Thermoelectric Power Factor of  $\text{LaOBiS}_{2-x}\text{Sex}$ . *J. Phys. Soc. Jpn.* **2016**, *85*, 074702. [[CrossRef](#)]
84. Kurematsu, K.; Ochi, M.; Usui, H.; Kurok, K. First-principles Study of  $\text{LaOPbBiS}_3$  and Its Analogous Compounds as Thermoelectric Materials. *J. Phys. Soc. Jpn.* **2020**, *89*, 024702. [[CrossRef](#)]
85. Morice, C.; Artacho, E.; Dutton, S.E.; Kim, H.J.; Saxena, S.S. Electronic and magnetic properties of superconducting  $\text{LnO}_{1-x}\text{FxBiS}_2$  (Ln = La, Ce, Pr, and Nd) from first principles. *J. Phys.-Condes. Matter* **2016**, *28*, 345504. [[CrossRef](#)]
86. Mejía-Salazar, J.R.; Perea, J.D.; Castillo, R.; Dioso J., E.; Baca, E. Hybrid Superconducting-Ferromagnetic  $[\text{Bi}_2\text{Sr}_2(\text{Ca},\text{Y})_2\text{Cu}_3\text{O}_{10}]_{0.99}(\text{La}_{2/3}\text{Ba}_{1/3}\text{MnO}_3)_{0.01}$  Composite Thick Films. *Materials* **2019**, *12*, 861. [[CrossRef](#)]
87. Rouco, V.; Córdoba, R.; De Teresa, J.M.; Rodríguez, L.A.; Navau, C.; Del-Valle, N.; Via, G.; Sánchez, A.; Monton, C.; Kronast, F.; et al. Competition between Superconductor-Ferromagnetic stray magnetic fields in  $\text{YBa}_2\text{Cu}_3\text{O}_{7-x}$  films pierced with Co nano-rods. *Sci. Rep.* **2017**, *7*, 5663. [[CrossRef](#)]
88. Zhang, G.; Samuely, T.; Xu, Z.; Jochum, J.K.; Volodin, A.; Zhou, S.; May, P.W.; Onufriienko, O.; Kacmarčík, J.; Steele, J.A.; et al. Superconducting Ferromagnetic Nanodiamond. *ACS Nano* **2017**, *11*, 5358–5366. [[CrossRef](#)]
89. Izumi, F.; Momma, K. Three-Dimensional Visualization in Powder Diffraction. *Solid State Phenom.* **2007**, *130*, 15. [[CrossRef](#)]
90. Momma, K.; Izumi, F. VESTA: A three-dimensional visualization system for electronic and structural analysis. *J. Appl. Crystallogr.* **2008**, *41*, 653. [[CrossRef](#)]



© 2020 by the authors. Licensee MDPI, Basel, Switzerland. This article is an open access article distributed under the terms and conditions of the Creative Commons Attribution (CC BY) license (<http://creativecommons.org/licenses/by/4.0/>).